

# Thermal effects on $\rho$ meson properties in an arbitrary magnetic field

Snigdha Ghosh<sup>a,c,\*</sup>, Arghya Mukherjee<sup>b,c,†</sup>, Mahatsab Mandal<sup>b,‡</sup>, Sourav Sarkar<sup>a,c,§</sup> and Pradip Roy<sup>b,c,¶</sup>

<sup>a</sup>Variable Energy Cyclotron Centre 1/AF Bidhannagar, Kolkata 700 064, India

<sup>b</sup>Saha Institute of Nuclear Physics, 1/AF Bidhannagar Kolkata - 700064, India and

<sup>c</sup>Homi Bhabha National Institute, Training School Complex, Anushaktinagar, Mumbai - 400085, India

Taking an effective  $\rho\pi\pi$  interaction, the self energy of  $\rho$  at finite temperature in an arbitrary external magnetic field is calculated using the real time formalism of thermal field theory. The effect of temperature and magnetic field on the in-medium spectral functions are studied. The effective mass and dispersion relations are evaluated from the pole of the complete  $\rho$  propagator. We find significant effects of magnetic field as well as temperature on self energies, spectral functions, effective masses and dispersion relations.

## I. INTRODUCTION

Recent researches in Quantum Chromodynamics(QCD) in presence of a very strong magnetic background have revealed remarkable properties of strong interaction [1]. From anomalous Chiral Magnetic Effect (CME), Chiral Vortical Effect to Magnetic Catalysis(MC), Inverse Magnetic Catalysis(IMC) and vacuum superconductivity, these non-trivial interplay between the topology, symmetry and anomaly [2–9] have enriched the fundamental aspects of QCD to a great extent. On one hand, noticeable influence on the strongly interacting sector can be achieved only when the background magnetic field is strong enough to be comparable to QCD scale i.e  $eB \approx m_\pi^2$ , on the other hand, non-central heavy-ion collisions in Relativistic Heavy-Ion Collider(RHIC) and Large Hadron Collider(LHC) can generate magnetic fields of  $eB \approx 15m_\pi^2$  [10]. Apart from its own theoretical intricacies, this promising platform for experimental manifestations has been one of the key reason for ensuing interests in this field of research. Moreover, similar environment inside the core of a magnetars adds to its astrophysical and cosmological importance [11–18].

A large amount of progress has been achieved in solving the so called puzzle of MC and IMC using the effective models most of which are focused on considering magnetic field dependent coupling constants or other magnetic field dependent parameters of the model (see for example [19]). One of the important method in extracting the information of  $eB$  dependencies of the chiral phase transition is to study the modifications of hadronic and mesonic properties in presence of medium/density along with external magnetic field. Moreover, mesons are more directly related to the chiral phase transition [20]. In this paper we mainly focus on the medium and temperature modifications of  $\rho$  meson in presence of homogeneous magnetic background. The study of the  $\rho$  meson properties like the effective mass and dispersion relations are important in the context of magnetic field induced vacuum superconductivity [9, 21–27]. It should be mentioned here that the dilepton production rate in heavy-ion collisions is directly proportional to the in-medium  $\rho$  spectral function and is well studied at vanishing magnetic field in Ref. [28–31]. However, the existence of such high external magnetic field in non central collisions should affect the spectral function of  $\rho$ . Thus the detailed study of the in-medium spectral properties of  $\rho$  meson in presence of  $eB$  may prove to be indispensable for analyzing the results of heavy-ion collision experiments.

Most of the calculations of one loop self energy functions at finite temperature under external magnetic field present in the literature employs strong/weak magnetic field approximation [32–34]. A few of them have relaxed this approximation and calculations are presented for arbitrary value of magnetic field like in Ref. [35, 36]. In the later case, even though the full Schwinger propagator for the loop particles are taken, yet the real part of the self energy is deprived of the magnetic field dependent vacuum contribution. In this work we have taken the full Schwinger propagator for the loop particles and do not make any approximations on the magnitude of the magnetic field. We have also considered the magnetic field dependent vacuum contributions to the real part of the self energy.

In Sec. II the vacuum self energy of  $\rho$  is given followed by evaluation of the in-medium  $\rho$  self-energy at zero magnetic field in Sec. III. Next in Sec. IV, the in-medium self energy at non-zero external magnetic field is presented. Sec. V is devoted to the discussion of the analytic structure of the self energy functions. In Sec. VI, the numerical results

---

\*Electronic address: snigdha.physics@gmail.com

†Electronic address: arghya.mukherjee@saha.ac.in

‡Electronic address: mahatsab@gmail.com

§Electronic address: sourav@vecc.gov.in

¶Electronic address: pradipk.roy@saha.ac.in

are shown and discussed. Finally we summarize and conclude in Sec. VII. Some of the relevant calculation details are given in the Appendix.

## II. $\rho$ SELF ENERGY IN THE VACUUM

The lowest order (LO) Lagrangian for effective  $\rho\pi\pi$  interaction can be written as [31]

$$\mathcal{L}_{int} = -g_{\rho\pi\pi}\partial_\mu\vec{\rho}_\nu \cdot \partial^\mu\vec{\pi} \times \partial^\nu\vec{\pi}, \quad (1)$$

with the effective coupling constant  $g_{\rho\pi\pi} = 20.72 \text{ GeV}^{-2}$ , which is fixed from the vacuum  $\rho \rightarrow \pi\pi$  decay width  $\Gamma_{\rho \rightarrow \pi\pi} = 150 \text{ MeV}$ .

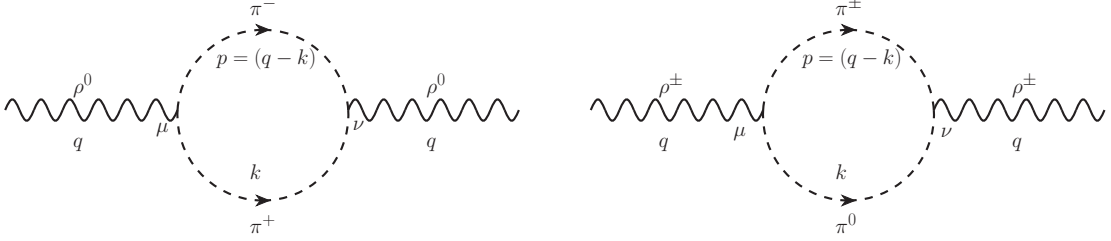


FIG. 1: Feynman diagrams for  $\rho$  self energy.

Using  $\mathcal{L}_{int}$ , the vacuum self energies of  $\rho^0$  and  $\rho^\pm$  are found to be (applying Feynman rules to Fig. 1),

$$(\Pi_0^{\mu\nu}(q))_{vac} = i \int \frac{d^4k}{(2\pi)^4} \mathcal{N}^{\mu\nu}(q, k) \Delta_\pm(k) \Delta_\pm(p) \quad (2)$$

$$(\Pi_\pm^{\mu\nu}(q))_{vac} = i \int \frac{d^4k}{(2\pi)^4} \mathcal{N}^{\mu\nu}(q, k) \Delta_0(k) \Delta_\pm(p) \quad (3)$$

respectively. In Eqs. (2) and (3),  $\Delta_0(k) = \left( \frac{-1}{k^2 - m_0^2 + i\epsilon} \right)$  and  $\Delta_\pm(k) = \left( \frac{-1}{k^2 - m_\pm^2 + i\epsilon} \right)$  are the vacuum Feynman propagators of  $\pi^0$  and  $\pi^\pm$  with masses  $m_0$  and  $m_\pm$  respectively and  $\mathcal{N}^{\mu\nu}(q, k)$  is given by,

$$\mathcal{N}^{\mu\nu}(q, k) = g_{\rho\pi\pi}^2 [q^4 k^\mu k^\nu + (q \cdot k)^2 q^\mu q^\nu - q^2 (q \cdot k) (q^\mu k^\nu + k^\mu q^\nu)], \quad (4)$$

which contains the factors coming from the interaction vertices. The momentum integrations in Eqs. (2) and (3) can be evaluated using standard Feynman parametrization followed by dimensional regularization. If we take  $m_0 = m_\pm = m_\pi$ , then the vacuum self energies of  $\rho^0$  and  $\rho^\pm$  are same and given by,

$$\Pi_{vac}^{\mu\nu}(q) = \left( \frac{q^2 g_{\rho\pi\pi}^2}{32\pi^2} \right) (q^2 g^{\mu\nu} - q^\mu q^\nu) \int_0^1 dx \Delta \left( \ln \frac{\Delta}{\mu_0} - 1 \right), \quad (5)$$

where  $\Delta = m^2 - x(1-x)q^2 - i\epsilon$  and  $\mu_0$  is a scale of dimension  $\text{GeV}^2$ . The metric tensor in this work is taken as  $g^{\mu\nu} = \text{diag}(1, -1, -1, -1)$ .

## III. $\rho$ SELF ENERGY IN THE MEDIUM

In the real time formalism of thermal field theory, the thermal propagators as well as the thermal self energies become  $2 \times 2$  matrices [30, 37]. However, they can be diagonalized in terms of a single analytic function which is related to any one component of the corresponding  $2 \times 2$  matrix, say the 11-component. The 11-component of the  $\pi^0$  and  $\pi^\pm$  thermal propagators are given by,

$$D_0^{11}(k) = \Delta_0(k) + 2i\eta^k \text{Im} \Delta_0(k) \quad (6)$$

$$D_\pm^{11}(k) = \Delta_\pm(k) + 2i\eta^k \text{Im} \Delta_\pm(k) \quad (7)$$

where,  $\eta^k = [e^{k \cdot u/T} - 1]^{-1}$  is the Bose-Einstein distribution function of the pions with  $u^\mu$  being the medium four-velocity. In local rest frame of the medium,  $u^\mu \equiv (1, \vec{0})$ . The complete in-medium vector matrix propagator  $\mathbf{D}^{\mu\nu}$  satisfies the following Dyson-Schwinger equation,

$$\mathbf{D}^{\mu\nu} = \Delta^{\mu\nu} - \Delta^{\mu\alpha} \Pi_{\alpha\beta} \mathbf{D}^{\beta\nu} \quad (8)$$

where,  $\Delta^{\mu\nu}$  is the free thermal vector matrix propagator and  $\Pi_{\alpha\beta}$  is the 1-loop thermal self energy matrix. Each of the quantities in Eq. (8) can be expressed in diagonal form in terms of analytic functions denoted by a bar, so that it can be written as,

$$\bar{D}^{\mu\nu} = \bar{\Delta}^{\mu\nu} - \bar{\Delta}^{\mu\alpha} \bar{\Pi}_{\alpha\beta} \bar{D}^{\beta\nu}. \quad (9)$$

The self energy function  $\bar{\Pi}_{\alpha\beta}$  is related to the 11-component of  $\Pi_{\alpha\beta}$  by the following relation,

$$\text{Re } \bar{\Pi}_{\alpha\beta}(q) = \text{Re } \Pi_{\alpha\beta}^{11}(q) \quad (10)$$

$$\text{Im } \bar{\Pi}_{\alpha\beta}(q) = \epsilon(q^0) \tanh\left(\frac{q^0}{2T}\right) \text{Im } \Pi_{\alpha\beta}^{11} \quad (11)$$

where,  $\epsilon(q^0) = 1$  for  $q^0 > 0$  and  $\epsilon(q^0) = -1$  for  $q^0 < 0$ . In order to obtain the 11-component of the  $\rho^0$  and  $\rho^\pm$  self energies, one has to replace the vacuum  $\pi^0$  and  $\pi^\pm$  propagators in Eq. (2) and (3) by their corresponding 11-component as given in Eqs. (6) and (7),

$$(\Pi_0^{\mu\nu}(q))^{11} = i \int \frac{d^4 k}{(2\pi)^4} \mathcal{N}^{\mu\nu}(q, k) D_\pm^{11}(k) D_\pm^{11}(p) \quad (12)$$

$$(\Pi_\pm^{\mu\nu}(q))^{11} = i \int \frac{d^4 k}{(2\pi)^4} \mathcal{N}^{\mu\nu}(q, k) D_0^{11}(k) D_\pm^{11}(p). \quad (13)$$

Performing the  $k^0$  integral and using Eqs. (10) and (11) we get the thermal self energy functions of  $\rho^0$  and  $\rho^\pm$  which are same if we take  $m_0 = m_\pm = m_\pi$ ,

$$\begin{aligned} \text{Re } \bar{\Pi}^{\mu\nu}(q) = \text{Re } \Pi_{vac}^{\mu\nu}(q) + \int \frac{d^3 k}{(2\pi)^3} \frac{1}{2\omega_k \omega_p} \mathcal{P} \left[ \left( \frac{\eta^k \omega_p \mathcal{N}^{\mu\nu}(k^0 = \omega_k)}{(q_0 - \omega_k)^2 - \omega_p^2} \right) + \left( \frac{\eta^k \omega_p \mathcal{N}^{\mu\nu}(k^0 = -\omega_k)}{(q_0 + \omega_k)^2 - \omega_p^2} \right) + \right. \\ \left. \left( \frac{\eta^p \omega_k \mathcal{N}^{\mu\nu}(k^0 = q_0 - \omega_p)}{(q_0 - \omega_p)^2 - \omega_k^2} \right) + \left( \frac{\eta^p \omega_k \mathcal{N}^{\mu\nu}(k^0 = q_0 + \omega_p)}{(q_0 + \omega_p)^2 - \omega_k^2} \right) \right] \end{aligned}$$

$$\begin{aligned} \text{Im } \bar{\Pi}^{\mu\nu}(q) = -\pi \epsilon(q_0) \int \frac{d^3 k}{(2\pi)^3} \frac{1}{4\omega_k \omega_p} \left[ \mathcal{N}^{\mu\nu}(k^0 = \omega_k) \{ (1 + \eta^k + \eta^p) \delta(q_0 - \omega_k - \omega_p) + (-\eta^k + \eta^p) \delta(q_0 - \omega_k + \omega_p) \} \right. \\ \left. + \mathcal{N}^{\mu\nu}(k^0 = -\omega_k) \{ (-1 - \eta^k - \eta^p) \delta(q_0 + \omega_k + \omega_p) + (\eta^k - \eta^p) \delta(q_0 + \omega_k - \omega_p) \} \right], \quad (14) \end{aligned}$$

where,  $\omega_k = \sqrt{\vec{k}^2 + m_\pi^2}$  and  $\omega_p = \sqrt{\vec{p}^2 + m_\pi^2} = \sqrt{(\vec{q} - \vec{k})^2 + m_\pi^2}$ .

#### IV. $\rho$ SELF ENERGY IN THE MEDIUM UNDER EXTERNAL MAGNETIC FIELD

In presence of external magnetic field (in addition to finite temperature), the  $\pi^0$  propagator remains unaffected whereas the 11-component of  $\pi^\pm$  propagator becomes [35],

$$D_B^{11}(k) = \Delta_B(k) + 2i\eta^k \text{Im } \Delta_B(k),$$

where,  $\Delta_B(k)$  is the Schwinger proper time propagator for a scalar field [33, 38],

$$\Delta_B(k) = i \int_0^\infty \frac{ds}{\cos(eBs)} \exp \left[ is \left( k_\parallel^2 + k_\perp^2 \frac{\tan(eBs)}{eBs} - m_\pi^2 + i\epsilon \right) \right]. \quad (15)$$

It may be noted that, Eq. (15) represents the charged scalar propagator in momentum space. The corresponding coordinate space propagator contains a phase factor which is not translationally invariant. However with a suitable

choice of the gauge, the phase factor can be removed [39], and one can work with the momentum space propagator. In Eq. (15),  $e = |e|$  is the absolute electronic charge; the external magnetic field  $\vec{B} = B\hat{z}$  is taken along the +ve z-direction and correspondingly a four-vector  $k$  is decomposed into  $k = (k_{\parallel} + k_{\perp})$ , where  $k_{\parallel} \equiv (k^0, 0, 0, k_z)$  and  $k_{\perp} \equiv (0, k_x, k_y, 0)$ . The metric tensor  $g^{\mu\nu}$  is also decomposed into  $g^{\mu\nu} = g_{\parallel}^{\mu\nu} + g_{\perp}^{\mu\nu}$ , where  $g_{\parallel}^{\mu\nu} = \text{diag}(1, 0, 0, -1)$  and  $g_{\perp}^{\mu\nu} = \text{diag}(0, -1, -1, 0)$ . Performing the proper time integration in Eq. (15), one gets,

$$\Delta_B(k) = \sum_{l=0}^{\infty} \frac{-\phi_l(\alpha_k)}{k_{\parallel}^2 - m_l^2 + i\epsilon},$$

where

$$m_l = \sqrt{m_{\pi}^2 + (2l+1)eB}, \quad (16)$$

$\phi_l(\alpha_k) = 2(-1)^l L_l(2\alpha_k) e^{-\alpha_k}$ ,  $\alpha_k = -k_{\perp}^2/eB$  and  $L_l(x)$  is the Laguerre polynomial of order  $l$  with  $L_{-1}(x) = 0$ . Replacing  $D_{\pm}^{11} \rightarrow D_B^{11}$  in Eqs. (12) and (13), and following Eqs. (10) and (11), one gets the  $\rho^0$  and  $\rho^{\pm}$  self energy functions at finite temperature in external magnetic field as,

$$\bar{\Pi}_0^{\mu\nu} = (\Pi_0^{\mu\nu})_B + (\Pi_0^{\mu\nu})_{BT} \quad (17)$$

$$\bar{\Pi}_{\pm}^{\mu\nu} = (\Pi_{\pm}^{\mu\nu})_B + (\Pi_{\pm}^{\mu\nu})_{BT}. \quad (18)$$

In Eqs. (17) and (18), subscript “B” and “BT” denote purely magnetic field dependent and both magnetic field as well as temperature dependent contributions respectively. For the sake of simplicity in the analytic calculations, we have taken the rho meson four-momenta as  $q^{\mu} \equiv (q^0, 0, 0, q_z)$ . The calculations of the “B” terms i.e. the magnetic field dependent vacuum contributions are tedious and provided in the Appendix (A) and (B). However the calculations of the “BT” terms are simple and similar to the  $eB = 0$  case. We summarize the explicit forms of different terms in Eqs. (17) and (18) bellow. The expressions for the real parts of  $\rho^0$  self energy function are

$$\begin{aligned} \text{Re}(\Pi_0^{\mu\nu})_B &= \text{Re} \Pi_{vac}^{\mu\nu} + \left( \frac{g_{\rho\pi\pi}^2 q_{\parallel}^2}{32\pi^2} \right) \int_0^1 dx \left[ (q_{\parallel}^2 g_{\parallel}^{\mu\nu} - q_{\parallel}^{\mu} q_{\parallel}^{\nu}) \text{Re} \left( 2eB \ln \Gamma \left( \frac{\Delta}{2eB} + \frac{1}{2} \right) - \Delta \ln \frac{\Delta}{2eB} + \Delta \right) \right. \\ &\quad \left. + q_{\parallel}^2 g_{\perp}^{\mu\nu} \text{Re} \left( \frac{\Delta}{2} \Psi \left( \frac{\Delta}{2eB} + \frac{1}{2} \right) + \frac{1}{2} (\Delta + (2x-1)eB) \Psi \left( \frac{\Delta}{2eB} + \frac{1}{2} + x \right) - \Delta \ln \frac{\Delta}{2eB} \right) \right] \end{aligned} \quad (19)$$

$$\begin{aligned} \text{Re}(\Pi_0^{\mu\nu})_{BT} &= \sum_{l=0}^{\infty} \sum_{n=0}^{\infty} \int_{-\infty}^{\infty} \frac{dk_z}{2\pi} \frac{1}{2\omega_k^l \omega_p^n} \mathcal{P} \left[ \left( \frac{\eta_l^k \omega_p^n \mathcal{N}_{nl}^{\mu\nu}(k^0 = \omega_k^l)}{(q_0 - \omega_k^l)^2 - (\omega_p^n)^2} \right) + \left( \frac{\eta_l^k \omega_p^n \mathcal{N}_{nl}^{\mu\nu}(k^0 = -\omega_k^l)}{(q_0 + \omega_k^l)^2 - (\omega_p^n)^2} \right) + \right. \\ &\quad \left. \left( \frac{\eta_n^p \omega_k^l \mathcal{N}_{nl}^{\mu\nu}(k^0 = q_0 - \omega_p^n)}{(q_0 - \omega_p^n)^2 - (\omega_k^l)^2} \right) + \left( \frac{\eta_n^p \omega_k^l \mathcal{N}_{nl}^{\mu\nu}(k^0 = q_0 + \omega_p^n)}{(q_0 + \omega_p^n)^2 - (\omega_k^l)^2} \right) \right], \end{aligned}$$

while the imaginary part is

$$\begin{aligned} \text{Im} \bar{\Pi}_0^{\mu\nu} &= -\pi\epsilon(q_0) \sum_{l=0}^{\infty} \sum_{n=0}^{\infty} \int_{-\infty}^{\infty} \frac{dk_z}{2\pi} \frac{1}{4\omega_k^l \omega_p^n} \\ &\quad [\mathcal{N}_{nl}^{\mu\nu}(k^0 = \omega_k^l) \{ (1 + \eta_l^k + \eta_n^p) \delta(q_0 - \omega_k^l - \omega_p^n) + (-\eta_l^k + \eta_n^p) \delta(q_0 - \omega_k^l + \omega_p^n) \} \\ &\quad \mathcal{N}_{nl}^{\mu\nu}(k^0 = -\omega_k^l) \{ (-1 - \eta_l^k - \eta_n^p) \delta(q_0 + \omega_k^l + \omega_p^n) + (\eta_l^k - \eta_n^p) \delta(q_0 + \omega_k^l - \omega_p^n) \}]. \end{aligned} \quad (20)$$

For the charged  $\rho$  meson, the corresponding expressions are:

$$\begin{aligned} \text{Re}(\Pi_{\pm}^{\mu\nu})_B &= \text{Re} \Pi_{vac}^{\mu\nu} + \left( \frac{g_{\rho\pi\pi}^2 q_{\parallel}^2}{32\pi^2} \right) \int_0^1 \int_0^1 dx dz z^{\Delta/m_{\pi}^2 - 1} \left[ (q_{\parallel}^2 g_{\parallel}^{\mu\nu} - q_{\parallel}^{\mu} q_{\parallel}^{\nu}) \left( \frac{\text{sech}(x \frac{eB}{m^2} \ln z)}{\tilde{\zeta} \ln z} - \frac{m^2}{(\ln z)^2} \right) \right. \\ &\quad \left. + q_{\parallel}^2 g_{\perp}^{\mu\nu} \left( \frac{1}{\tilde{\zeta} m^2} - \frac{m^2}{(\ln z)^2} \right) \right] \end{aligned} \quad (21)$$

$$\begin{aligned}
\text{Re}(\Pi_{\pm}^{\mu\nu})_{BT} &= \sum_{n=0}^{\infty} \int \frac{d^3k}{(2\pi)^3} \frac{\phi_n(\alpha_k)}{2\omega_k\omega_p^n} \mathcal{P} \left[ \left( \frac{\eta^k \omega_p^n \mathcal{N}^{\mu\nu}(k^0 = \omega_k)}{(q_0 - \omega_k)^2 - (\omega_p^n)^2} \right) + \left( \frac{\eta^k \omega_p^n \mathcal{N}^{\mu\nu}(k^0 = -\omega_k)}{(q_0 + \omega_k)^2 - (\omega_p^n)^2} \right) \right. \\
&\quad \left. + \left( \frac{\eta_p^n \omega_k \mathcal{N}^{\mu\nu}(k^0 = q_0 - \omega_p^n)}{(q_0 - \omega_p^n)^2 - (\omega_k)^2} \right) + \left( \frac{\eta_p^n \omega_k \mathcal{N}^{\mu\nu}(k^0 = q_0 + \omega_p^n)}{(q_0 + \omega_p^n)^2 - (\omega_k)^2} \right) \right] \\
\text{Im } \bar{\Pi}_{\pm}^{\mu\nu} &= -\pi\epsilon(q_0) \sum_{n=0}^{\infty} \int \frac{d^3k}{(2\pi)^3} \frac{\phi_n(\alpha_k)}{4\omega_k\omega_p^n} \\
&\quad [\mathcal{N}^{\mu\nu}(k^0 = \omega_k) \{ (1 + \eta^k + \eta_p^n) \delta(q_0 - \omega_k - \omega_p^n) + (-\eta^k + \eta_p^n) \delta(q_0 - \omega_k + \omega_p^n) \} \\
&\quad \mathcal{N}^{\mu\nu}(k^0 = -\omega_k) \{ (-1 - \eta^k - \eta_p^n) \delta(q_0 + \omega_k + \omega_p^n) + (\eta^k - \eta_p^n) \delta(q_0 + \omega_k - \omega_p^n) \}] , \tag{22}
\end{aligned}$$

where,  $\Psi(z)$  is the digamma function,  $\tilde{\zeta} = (1-x) \frac{1}{m_\pi^2} \ln z + \frac{1}{eB} \tanh\left(x \frac{eB}{m_\pi^2} \ln z\right)$ ,  $\omega_k^l = \sqrt{k_z^2 + m_l^2}$ ,  $\eta_k^l = \left[e^{\omega_k^l/T} - 1\right]^{-1}$  and

$$\begin{aligned}
\mathcal{N}_{nl}^{\mu\nu}(q_{\parallel}, k_{\parallel}) &= \frac{g_{\rho\pi\pi}^2}{2} (-1)^{n+l} \left( \frac{eB}{\pi} \right) \left[ q_{\parallel}^4 k_{\parallel}^{\mu} k_{\parallel}^{\nu} + (q_{\parallel} \cdot k_{\parallel})^2 q_{\parallel}^{\mu} q_{\parallel}^{\nu} - q_{\parallel}^2 (q_{\parallel} \cdot k_{\parallel}) (q_{\parallel}^{\mu} k_{\parallel}^{\nu} + k_{\parallel}^{\mu} q_{\parallel}^{\nu}) \right] \delta_{n,l} \\
&\quad - \frac{g_{\rho\pi\pi}^2}{8} eB q_{\parallel}^4 g_{\perp}^{\mu\nu} \left[ (2n+1) \delta_{n,l} - n \delta_{n-1,l} - (n+1) \delta_{n+1,l} \right] . \tag{23}
\end{aligned}$$

## V. ANALYTIC STRUCTURE OF THE IMAGINARY PARTS

Each of the imaginary parts of the self energy functions in Eqs. (14), (20) and (22) contains four Dirac delta functions which will give rise to branch cuts of the self energy function in the complex  $q^0$  plane, details of which are provided in Appendix C. Let us first discuss the analytic structure at finite temperature in absence of magnetic field. In Eq. 14, the first term containing  $\delta(q^0 - \omega_k - \omega_p)$  is non vanishing for  $\sqrt{\vec{q}^2 + 4m_\pi^2} < q^0 < \infty$  and we call this “Unitary-I” cut. The second term containing  $\delta(q^0 - \omega_k + \omega_p)$  is non vanishing for  $-|\vec{q}| < q^0 < 0$  and this is the “Landau-II” cut. The third term containing  $\delta(q^0 + \omega_k + \omega_p)$  is non vanishing for  $-\infty < q^0 < -\sqrt{\vec{q}^2 + 4m_\pi^2}$  and we call this is “Unitary-II” cut. Finally the fourth term containing  $\delta(q^0 + \omega_k - \omega_p)$  is non vanishing for  $0 < q^0 < |\vec{q}|$  and this is the “Landau-I” cut. These different cuts are shown in Fig. 2 and correspond to different physical processes. We are interested in the physical kinematic region  $q^0 > 0$  and  $q^2 > 0$ . In this region Unitary-I and Landau-I terms contribute. Unitary-I cut corresponds to the decay of a  $\rho$  into two pions which can also happen in vacuum, whereas the Landau-I cut is purely a medium effect which corresponds to the absorption of a  $\rho$  due to scattering with a  $\pi$  producing a  $\pi$  in the final state. If we take  $\vec{q} = \vec{0}$ , then the Landau contributions will be absent and we are left with only Unitary cut contributions.

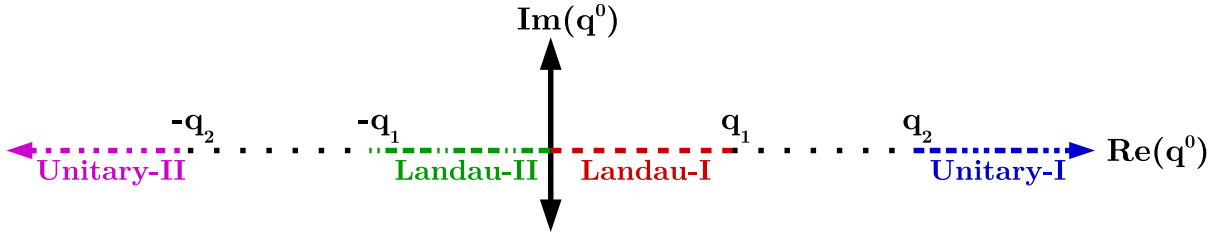


FIG. 2: Different branch cuts of the in-medium self energy function at *zero magnetic field* of the  $\rho$  in the complex  $q^0$  plane for a given  $\vec{q}$ . The points correspond to  $q_1 = |\vec{q}|$  and  $q_2 = \sqrt{\vec{q}^2 + 4m_\pi^2}$ .

Let us now turn on the magnetic field. The imaginary part of  $\rho^0$  self energy function in presence of the external magnetic field in Eq. (20) is non vanishing at four different kinematic regions. Note that in this case the quantity  $m_l$  in Eq. (16) for charged pions in the loop contains a contribution from the transverse momentum component which are quantized. As shown in Appendix C, the Unitary-I and Unitary-II cuts are defined in  $\sqrt{\vec{q}_z^2 + 4(m_\pi^2 + eB)} < q^0 < \infty$  and  $-\infty < q^0 < -\sqrt{\vec{q}_z^2 + 4(m_\pi^2 + eB)}$  respectively, whereas both the Landau-I and Landau-II cuts are defined in

$|q^0| < \sqrt{q_z^2 + (\sqrt{m_\pi^2 + eB} - \sqrt{m_\pi^2 + 3eB})^2}$ . These cuts are shown in Fig. 3. It is to be noted that, in presence of the external magnetic field, the in-medium  $\rho^0$  self energy always possesses the Landau contribution even if  $\vec{q} = \vec{0}$ .

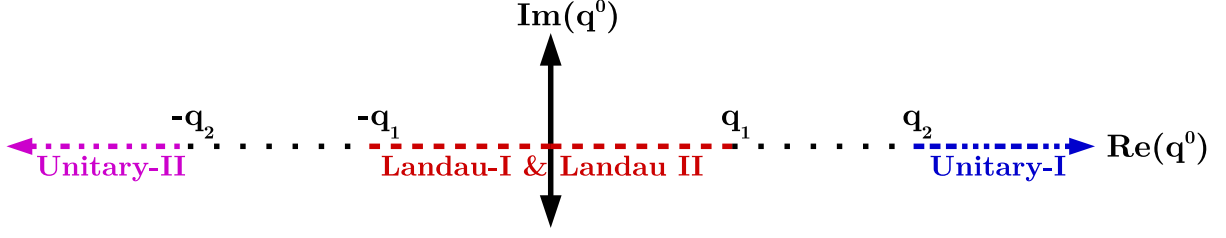


FIG. 3: Different branch cuts of the in-medium self energy function under external magnetic field of the  $\rho^0$  in the complex  $q^0$  plane for a given  $\vec{q}$ . The points correspond to  $q_1 = \sqrt{q_z^2 + (\sqrt{m_\pi^2 + eB} - \sqrt{m_\pi^2 + 3eB})^2}$  and  $q_2 = \sqrt{q_z^2 + 4(m_\pi^2 + eB)}$ .

In a similar way, the imaginary part of  $\rho^\pm$  self energy function in presence of the external magnetic field in Eq. (22) has its Unitary-I and Unitary-II cuts in the kinematic domain  $\sqrt{q_z^2 + (\sqrt{m_\pi^2 + eB} + m_\pi)^2} < q^0 < \infty$  and  $-\infty < q^0 < -\sqrt{q_z^2 + (\sqrt{m_\pi^2 + eB} + m_\pi)^2}$  respectively, whereas it has its Landau-I and Landau-II cuts in the kinematic domain  $0 < q^0 < \infty$  and  $-\infty < q^0 < 0$  respectively. These cuts are displayed in Fig. 4. In this case also the in-medium  $\rho^\pm$  self energy always has a finite Landau cut contribution even if  $\vec{q} = \vec{0}$ .

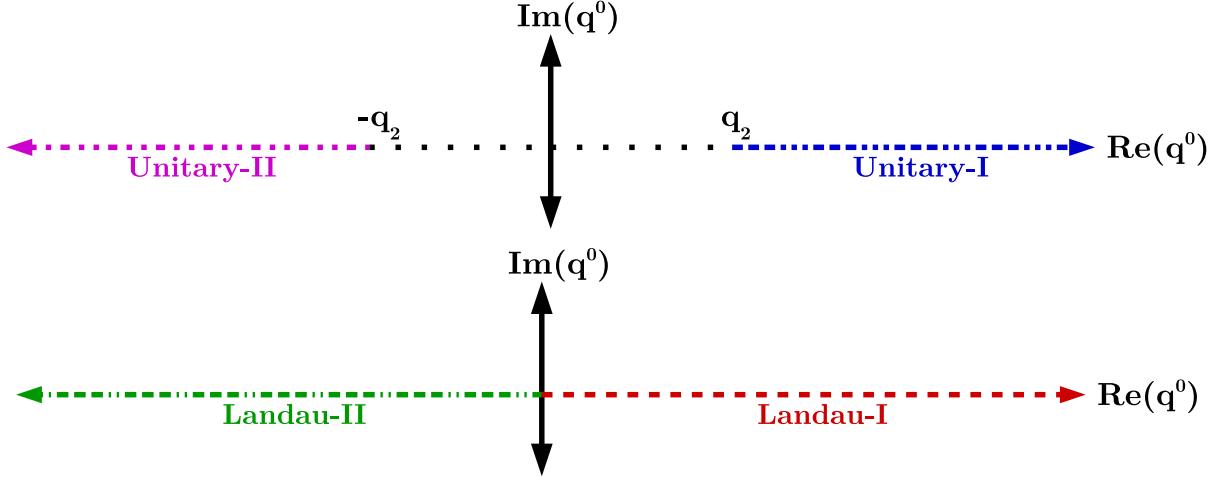


FIG. 4: Different branch cuts of the in-medium self energy functions under external magnetic field of the  $\rho^\pm$  in the complex  $q^0$  plane for a given  $\vec{q}$ . Upper-Panel shows the Unitary cut regions with  $q_2 = \sqrt{q_z^2 + (\sqrt{m_\pi^2 + eB} + m_\pi)^2}$ . Lower-Panel shows the Landau cut regions.

The imaginary parts given in Eq. (14),(20) and (22) have been further simplified using the Dirac delta functions present in the integrand. For simplicity, the expressions for  $\vec{q} = \vec{0}$  are presented here and can be obtained from Appendix (D),

$$\text{Im } \bar{\Pi}^{\mu\nu}(q^0, \vec{q} = \vec{0}) = \left( \frac{-\epsilon(q^0)\tilde{k}}{8\pi q^0} \right) \left[ U_1(q^0, |\vec{k}| = \tilde{k}) \Theta(q^0 - 2m_\pi) + U_2(q^0, |\vec{k}| = \tilde{k}) \Theta(-q^0 - 2m_\pi) \right] \quad (24)$$

$$\begin{aligned} \text{Im } \bar{\Pi}_0^{\mu\nu}(q^0, \vec{q} = \vec{0}) = & \left( \frac{-\epsilon(q^0)}{4|q^0|} \right) \sum_{l=0}^{\infty} \sum_{n=0}^{\infty} \frac{1}{\tilde{k}_z} \left[ U_1^{n,l}(q^0, \tilde{k}_z) \Theta(q^0 - m_l - m_n) + U_2^{n,l}(q^0, \tilde{k}_z) \Theta(-q^0 - m_l - m_n) \right. \\ & + L_1^{n,l}(q^0, \tilde{k}_z) \Theta(-q^0 - \min(m_l - m_n, 0)) \Theta(\max(m_l - m_n, 0) + q^0) \\ & \left. + L_2^{n,l}(q^0, \tilde{k}_z) \Theta(q^0 - \min(m_l - m_n, 0)) \Theta(\max(m_l - m_n, 0) - q^0) \right] \quad (25) \end{aligned}$$

$$\begin{aligned} \text{Im } \bar{\Pi}_{\pm}^{\mu\nu}(q^0, \vec{q} = \vec{0}) = & \left( \frac{-\epsilon(q^0)}{16\pi} \right) \sum_{n=0}^{\infty} \left[ \int_{\omega_-}^{\omega_0} \frac{d\omega_k}{|\vec{k}| \cos \theta_0} \left( U_1^n(q^0, |\vec{k}|, \theta_0) + U_1^n(q^0, |\vec{k}|, -\theta_0) \right) \Theta(q^0 - m_\pi - m_n) \right. \\ & + \int_{-\omega_+}^{-\omega_0} \frac{d\omega_k}{|\vec{k}| \cos \theta'_0} \left( U_2^n(q^0, |\vec{k}|, \theta'_0) + U_2^n(q^0, |\vec{k}|, -\theta'_0) \right) \Theta(-q^0 - m_\pi - m_n) \\ & + \int_{\omega_0}^{\omega_+} \frac{d\omega_k}{|\vec{k}| \cos \theta'_0} \left( L_1^n(q^0, |\vec{k}|, \theta'_0) + L_1^n(q^0, |\vec{k}|, -\theta'_0) \right) \Theta(-q^0 - m_\pi + m_n) \Theta(q^0) \\ & \left. + \int_{-\omega_0}^{-\omega_-} \frac{d\omega_k}{|\vec{k}| \cos \theta_0} \left( L_2^n(q^0, |\vec{k}|, \theta_0) + L_2^n(q^0, |\vec{k}|, -\theta_0) \right) \Theta(q^0 - m_\pi + m_n) \Theta(-q^0) \right] \quad (26) \end{aligned}$$

where,  $\omega_{\pm} = (q^0 \pm m_n)$  and  $\omega_0 = \frac{1}{2q^0} (q_0^2 + m_\pi^2 - m_n^2)$ . The Lorentz indices  $\mu, \nu$  are contained in  $U_{1,2}$  and  $L_{1,2}$  (see Appendix C).

## VI. NUMERICAL RESULTS

We begin our results by showing the imaginary and real part of the in-medium self energy functions of  $\rho$  under external magnetic field. We will present numerical results for the spin averaged quantity  $\Pi_{0,\pm} = \frac{1}{3} g_{\mu\nu} \bar{\Pi}_{0,\pm}^{\mu\nu}$ . First, we have checked numerically that in the limit  $eB \rightarrow 0$ , the  $eB = 0$  results ( $T \neq 0$ ) are exactly reproduced, i.e.

$$\lim_{eB \rightarrow 0} \bar{\Pi}_0^{\mu\nu} = \lim_{eB \rightarrow 0} \bar{\Pi}_{\pm}^{\mu\nu} = \bar{\Pi}^{\mu\nu}. \quad (27)$$

To take  $eB \rightarrow 0$  limit, numerically we have taken upto 300 Landau levels for a convergent result. However, for the other results presented here for  $eB \geq 0.05 \text{ GeV}^2$ , the results are well convergent with 200 Landau levels.

In Fig. 5, the Landau cut contributions for the imaginary parts of the self energy functions are shown. The spikes occurring in the upper panel for the  $\rho^0$  are due to the ‘‘Threshold Singularity’’ for each Landau level as can be understood from Eq. (25). In Eq. (25) we have a  $\tilde{k}_z$  present in the denominator which has appeared due to dimensional reduction in the  $\rho^0$  self energy. For a particular set of Landau levels  $\{n, l\}$ , we have

$$\tilde{k}_z = \frac{1}{2q^0} \lambda^{1/2} (q_0^2, m_l^2, m_n^2) = \frac{1}{2q^0} (q^0 + m_l + m_n) (q^0 - m_l - m_n) (q^0 + m_l - m_n) (q^0 - m_l - m_n),$$

which will go to zero at each threshold of Unitary and Landau cut defined in terms of the step functions in Eq. (25). This will give rise to the spike like structure in the upper panel. Physically the spikes correspond to the fluctuation of  $\rho^0$  into two pions occurring in the transverse plane with respect to the direction of external magnetic field. Moreover, at these threshold values of  $q^0$ , the  $\rho^0$  will be infinitely unstable and will decay into pions immediately. In Fig. 5(a) we have shown results for four different values of  $eB$  (0.05, 0.10, 0.15 and 0.20  $\text{GeV}^2$  respectively) at a constant temperature 160 MeV. As  $eB$  increases, the threshold of the Landau cuts move towards higher value of  $q^0$  as evident from Eq. (25). Also with the increase of  $eB$ , the separation among the spikes becomes larger. In Fig. 5(b), results are shown at a constant  $eB$  (0.10  $\text{GeV}^2$ ) and at three different values of temperatures (100, 130 and 160 MeV respectively). In this case the threshold remains unchanged but the magnitude becomes larger which is due to the increase of the thermal distribution functions with the increase of temperature.

In Fig. 5(c)-(d), similar results for the  $\rho^{\pm}$  are shown. In this case, there is no threshold for the Landau cuts and they extend from  $-\infty < q^0 < \infty$ . The oscillations are due to the presence of one Laguerre polynomial in Eq. (26). It is also to be noted that, at a higher value of  $eB$  the significant contributions start from a higher  $q^0$ . In Fig. 5(d), we

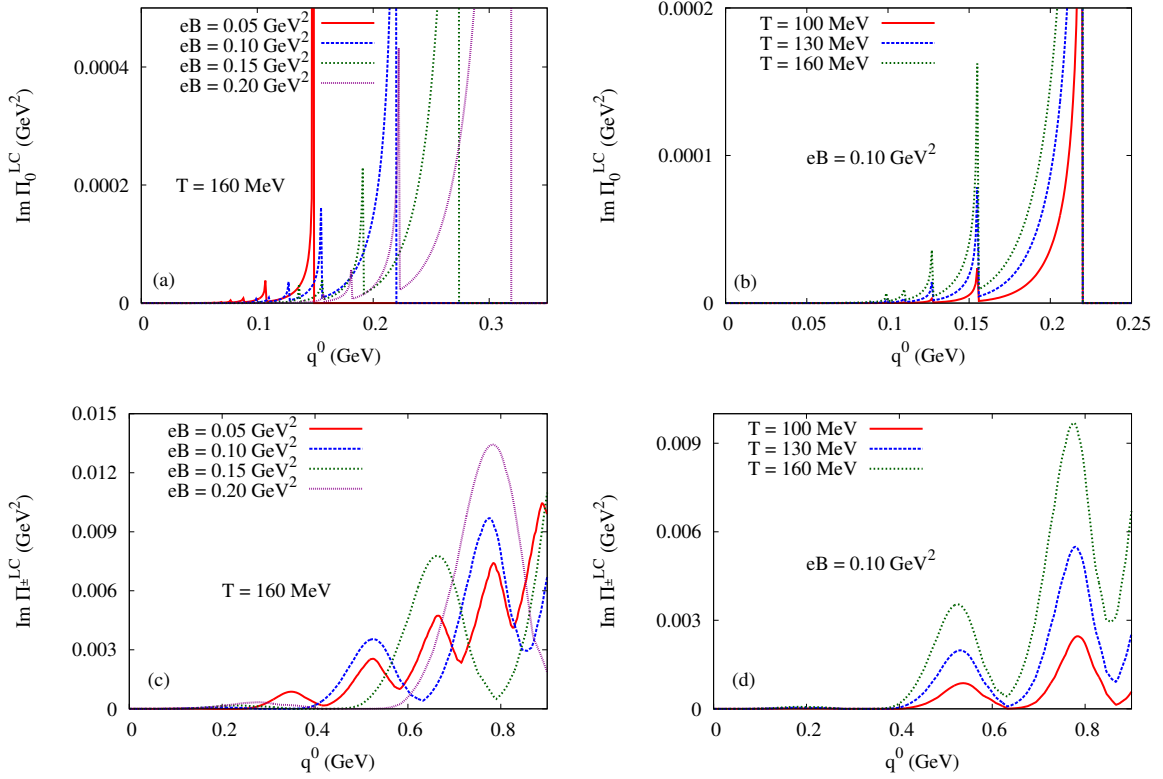


FIG. 5: The Landau cut contributions to the imaginary part of the self energy function of (a)  $\rho^0$  at constant temperature (160 MeV) and at four different values of the magnetic field (0.05, 0.10, 0.15 and 0.20  $\text{GeV}^2$  respectively), (b)  $\rho^0$  at constant magnetic field (0.01  $\text{GeV}^2$ ) and at three different values of the temperature (100, 130 and 160 MeV respectively), (c)  $\rho^\pm$  at constant temperature (160 MeV) and at four different values of the magnetic field (0.05, 0.10, 0.15 and 0.20  $\text{GeV}^2$  respectively) and (d)  $\rho^\pm$  at constant magnetic field (0.01  $\text{GeV}^2$ ) and at three different values of the temperature (100, 130 and 160 MeV respectively).

see that the magnitude of the imaginary parts increases with the increase in temperature keeping the overall structure unaltered which is due to increase in the thermal distribution function with the increase of temperature.

In Fig. 6 the Unitary cut contributions to the imaginary part of the self energy functions are presented. In Fig. 6(a), results for  $\rho^0$  at a constant temperature (160 MeV) and at four different values of the magnetic field (0.05, 0.10, 0.15 and 0.20  $\text{GeV}^2$  respectively) are shown. Similar to the Landau cut contribution, the Unitary cut contributions of  $\rho^0$  also suffer from the "Threshold Singularities". As the magnetic field increases, the threshold of the Unitary cuts moves towards higher  $q^0$  and the separations among the spikes increase. In Fig. 6(b), results are shown for a constant  $eB$  (0.10  $\text{GeV}^2$ ) and at three different values of the temperature (100, 130 and 160 MeV respectively). As the temperature increases, the magnitudes of the self energies increase keeping the thresholds unchanged similar to the Landau cut contributions. However, unlike the Landau contributions, the Unitary contributions are dominated by the vacuum contribution and the effect of increase of temperature is very small.

In Fig. 6(c)-(d), similar results are presented for the charged  $\rho$ . The  $\rho^\pm$  has different thresholds for the Unitary cuts than the  $\rho^0$  as given in Eq. (26). The displacement of the Unitary cut threshold towards higher  $q^0$  with the increase in  $eB$  is small as compared to that of  $\rho^0$  and this will have significant effect on the spectral functions. Small oscillation can be noticed in the graphs, which are due to the presence of a Laguerre polynomial. However these oscillations and the effect of temperature is very small as the Unitary cut is dominated by the vacuum contributions.

Next in Fig. 7, the real part of the in-medium self energy functions of  $\rho$  at non-zero external magnetic field are presented. In Fig. 7(a), results of the  $\rho^0$  at constant temperature (160 MeV) and at four different values of the magnetic field (0.05, 0.10, 0.15 and 0.20  $\text{GeV}^2$  respectively) are shown. These plots are dominated by the "B" terms in Eq. (17). Small oscillatory behaviour present in the plots due to the numerical principal value integrations. In Fig. 7(b), results are shown at a constant magnetic field (0.01  $\text{GeV}^2$ ) and at three different values of the temperature (100, 130 and 160 MeV respectively). Effects of the increase in temperature are small and makes the real part larger.



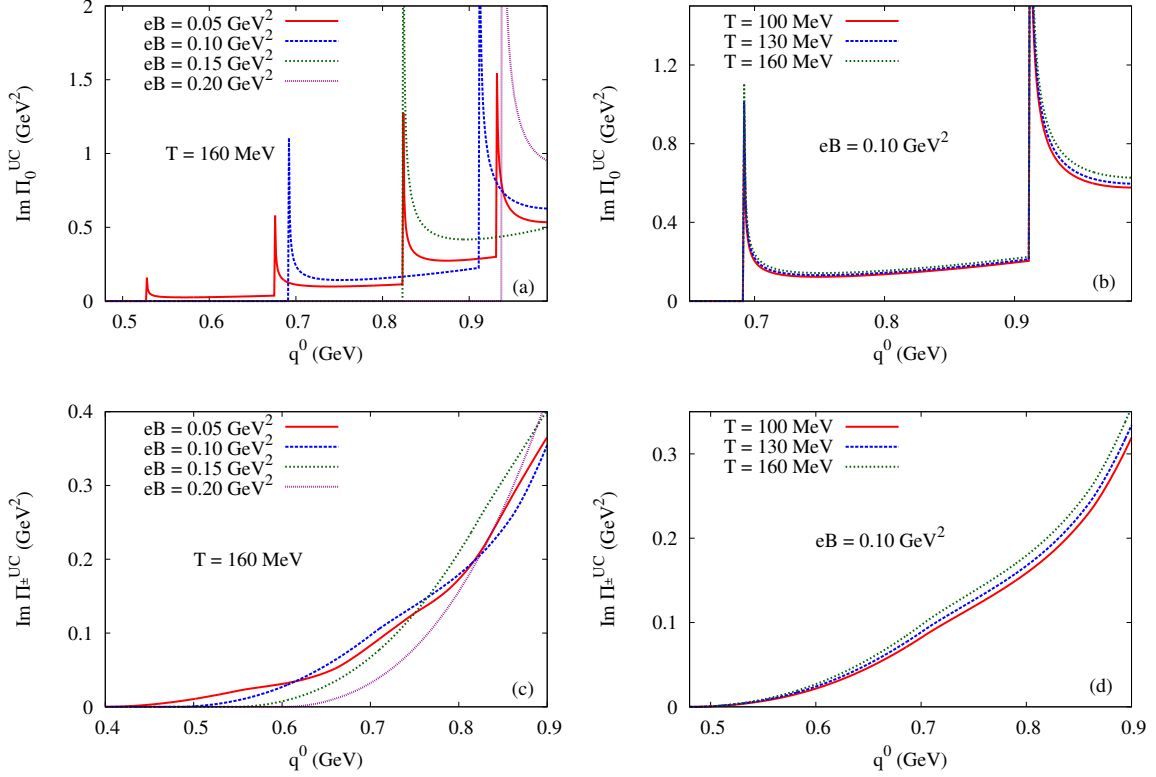


FIG. 6: The Unitary cut contributions to the imaginary part of the self energy function of (a)  $\rho^0$  at constant temperature (160 MeV) and at four different values of the magnetic field (0.05, 0.10, 0.15 and 0.20  $\text{GeV}^2$  respectively), (b)  $\rho^0$  at constant magnetic field (0.01  $\text{GeV}^2$ ) and at three different values of the temperature (100, 130 and 160 MeV respectively), (c)  $\rho^\pm$  at constant temperature (160 MeV) and at four different values of the magnetic field (0.05, 0.10, 0.15 and 0.20  $\text{GeV}^2$  respectively) and (d)  $\rho^\pm$  at constant magnetic field (0.01  $\text{GeV}^2$ ) and at three different values of the temperature (100, 130 and 160 MeV respectively).

Similar plots for  $\rho^\pm$  are presented in the lower panel. Fig. 8 shows the comparison of the real part of the self energy function between  $\rho^0$  and  $\rho^\pm$ . Results at two combinations of  $eB$  and  $T$  are given ( $eB=0.10 \text{ GeV}^2$ ,  $T=100 \text{ MeV}$  and  $eB=0.20 \text{ GeV}^2$ ,  $T=160 \text{ MeV}$  respectively). In both the cases, they have similar magnitude at lower value of  $q^0$  (with  $\rho^0$  a little lower). With the increase of  $q^0$  the  $\rho^0$  self energy crosses the  $\rho^\pm$  at a larger  $q^0$ .

Having obtained the real and imaginary parts we proceed to present the in-medium spectral functions of  $\rho$  which contains both the real and imaginary parts of the self energy function. The spectral function is the imaginary part of the complete propagator and defined as,

$$S_{0,\pm}(q^0, eB, T) = \frac{\text{Im } \Pi_{0,\pm}}{(q_0^2 - m_\rho^2 + \text{Re } \Pi_{0,\pm})^2 + (\text{Im } \Pi_{0,\pm})^2} \quad (28)$$

In Fig. 9, spectral functions of  $\rho^0$  are shown. In the upper panel, results are shown at constant temperature (160 MeV) and at three different values of the magnetic field (0.10, 0.15 and 0.20  $\text{GeV}^2$  respectively). The spectral functions have the same threshold as the imaginary parts of the self energy, as is evident from Eq. (28). The spectral functions are shown in two parts, Fig. 9(a) shows the lower  $q^0$  regions dominated by the Landau terms whereas Fig. 9(b) shows the higher  $q^0$  regions, dominated by Unitary terms. It is seen from Fig. 9(a) that, with the increase of the magnetic field, the threshold of the spectral function shifts towards higher  $q^0$ . However in Fig. 9(b) due to the displacement of the threshold towards higher  $q^0$ , with the increase in magnetic field, the spectral function misses the  $\rho$  mass pole, loses its Breit-Wigner shape, and becomes a continuum at large  $q^0$ . This physically implies the “melting” of the  $\rho^0$  at higher value of the magnetic field. In the lower panel, the spectral functions at constant  $eB$  (0.10  $\text{GeV}^2$ ) and at three different values of the temperature (100, 130 and 160 MeV respectively) are shown. The increase in temperature increases the magnitude of the spectral function at low  $q^0$  region and decreases the magnitude at higher  $q^0$  region without changing the threshold and shape.

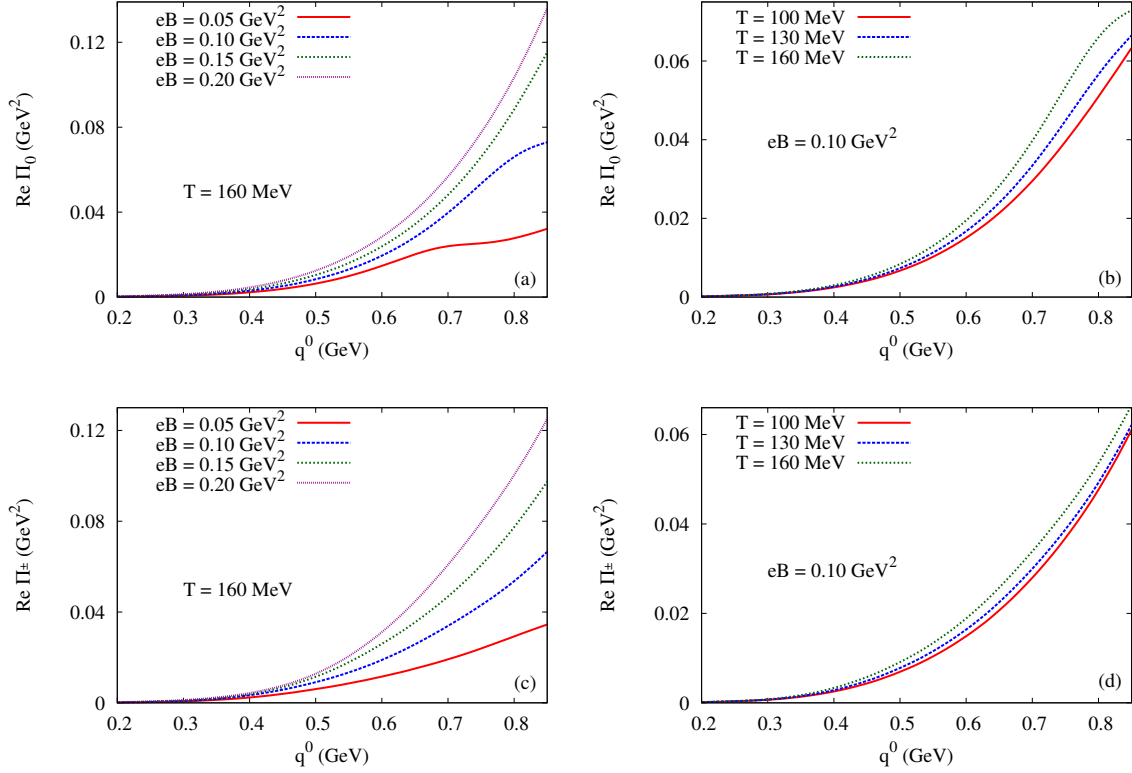


FIG. 7: The real part of the self energy function of (a)  $\rho^0$  at constant temperature (160 MeV) and at four different values of the magnetic field (0.05, 0.10, 0.15 and 0.20  $\text{GeV}^2$  respectively), (b)  $\rho^0$  at constant magnetic field (0.01  $\text{GeV}^2$ ) and at three different values of the temperature (100, 130 and 160 MeV respectively), (c)  $\rho^\pm$  at constant temperature (160 MeV) and at four different values of the magnetic field (0.05, 0.10, 0.15 and 0.20  $\text{GeV}^2$  respectively) and (d)  $\rho^\pm$  at constant magnetic field (0.01  $\text{GeV}^2$ ) and at three different values of the temperature (100, 130 and 160 MeV respectively).

In Fig. 10, similar plots of in-medium spectral function of  $\rho^\pm$  are shown. In Fig. 10(b), it is observed that with the increase in  $eB$ , the threshold of the spectral function has a displacement towards the higher  $q^0$ , however the rate of this displacement is slower as compared to the  $\rho^0$  case and the  $\rho$  mass pole is yet to be reached even at  $eB=0.20 \text{ GeV}^2$ . So the spectral functions maintains its Breit-Wigner shape intact even at a higher value of  $eB$ . However it causes squeezing of  $\rho^\pm$  width and making it more stable. But further increase of  $eB$  will cause “melting” of  $\rho^\pm$  as well. The effect of increase of temperature is similar to that of  $\rho^0$  and shown in lower panel. In Fig. 11, comparison of the  $\rho^0$  and  $\rho^\pm$  spectral functions are shown. Fig. 11(a) shows the lower  $q^0$  region and Fig. 11(b) shows the higher  $q^0$  region.

Now we turn our attention to the calculations of mass and dispersion relations. From the pole of the complete  $\rho$  propagator, the following dispersion relation is obtained

$$\det [(-q^2 + m_\rho^2) g^{\mu\nu} + q^\mu q^\nu - \text{Re } \bar{\Pi}_{0,\pm}^{\mu\nu}] = 0. \quad (29)$$

Effective mass( $m^*$ ) of  $\rho$  is calculated by putting  $\rho$  three-momentum  $\vec{q} = \vec{0}$  in the dispersion relation. Clearly, Eq. (29) will admit 4 solutions and we should get four modes of the effective mass and dispersion relation. However in this work, since we have taken  $\vec{q} = (0, 0, q_z)$ , we get three physical modes and of which two are identical. So we are left with two distinct modes. We call these modes as Mode-I and Mode-II respectively.

In Fig. 12 we have shown the results on effective mass the  $\rho$ . In Fig. 12(a),  $m^*$  of Mode-I is plotted against  $eB$  for  $\rho^0$  and  $\rho^\pm$  at two different temperatures (100 and 160 MeV respectively).  $m^*$  decreases significantly with the increase in  $eB$  due to a strong positive contribution coming from the real part of the self energy. Fig. 12(c),  $m^*$  is plotted against  $T$  at two different values of the magnetic field (0.05 and 0.10  $\text{GeV}^2$  respectively). The variation of  $m^*$  with  $T$  is slow as the contribution of the “BT” terms is small compared to the “B” terms as seen from Eqs. (17) and (18). Figs. 12(b) and 12(d) shows similar plots for Mode-II.

Finally, we have shown the dispersion curves of the  $\rho$  in Fig. 13 at a constant temperature (160 MeV) and at two

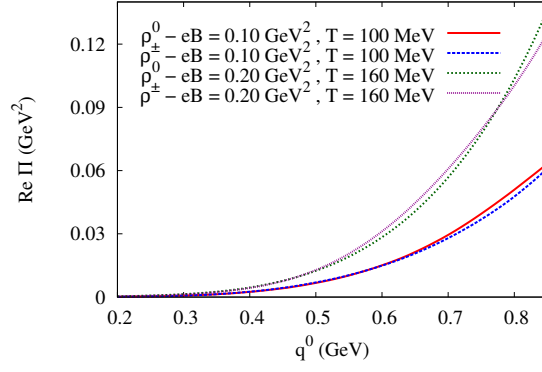


FIG. 8: The comparison of the real part of the self energy function between  $\rho^0$  and  $\rho^\pm$  at two different combinations of the magnetic field and temperature ( $eB=0.10 \text{ GeV}^2$ ,  $T=100 \text{ MeV}$  and  $eB=0.20 \text{ GeV}^2$ ,  $T=160 \text{ MeV}$  respectively).

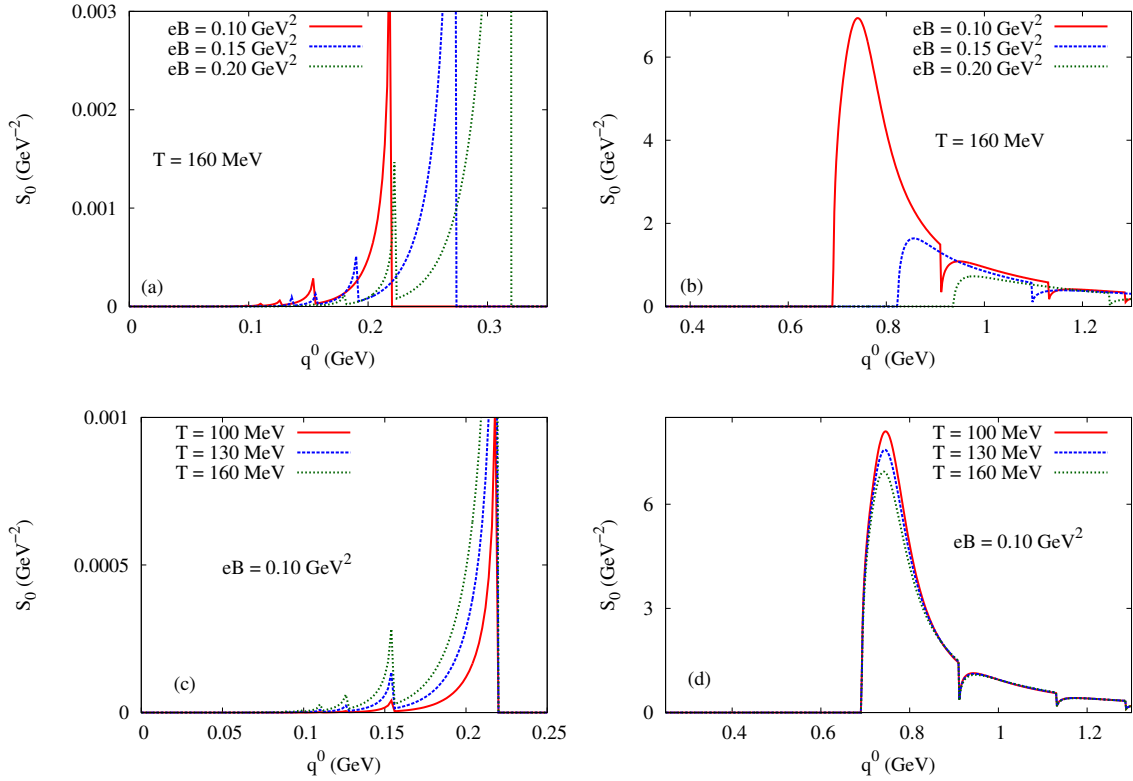


FIG. 9: The in-medium spectral functions of the  $\rho^0$  at constant temperature (160 MeV) and at three different values of the magnetic field (0.10, 0.15 and 0.20  $\text{GeV}^2$  respectively) (a) for  $q^0$  from 0 to 0.35 GeV (b) for  $q^0$  from 0.35 to 1.3 GeV (upper panel). The in-medium spectral functions of the  $\rho^0$  at constant magnetic field (0.10  $\text{GeV}^2$ ) and at three different values of the temperature (100, 130 and 160 MeV respectively) (c) for  $q^0$  from 0 to 0.25 GeV (d) for  $q^0$  from 0.25 to 1.3 GeV (lower panel).

different values of  $eB$  (0.10 and 0.20  $\text{GeV}^2$  respectively). The dispersion relations are well separated around  $q_z = 0$ . As we go towards higher and lower values of  $q_z$ , we reach the light-like dispersion relations as the corrections due to  $eB$  and/or  $T$  will be small. Figs. 13(a) and 13(b) shows results for Mode-I and Mode-II respectively.

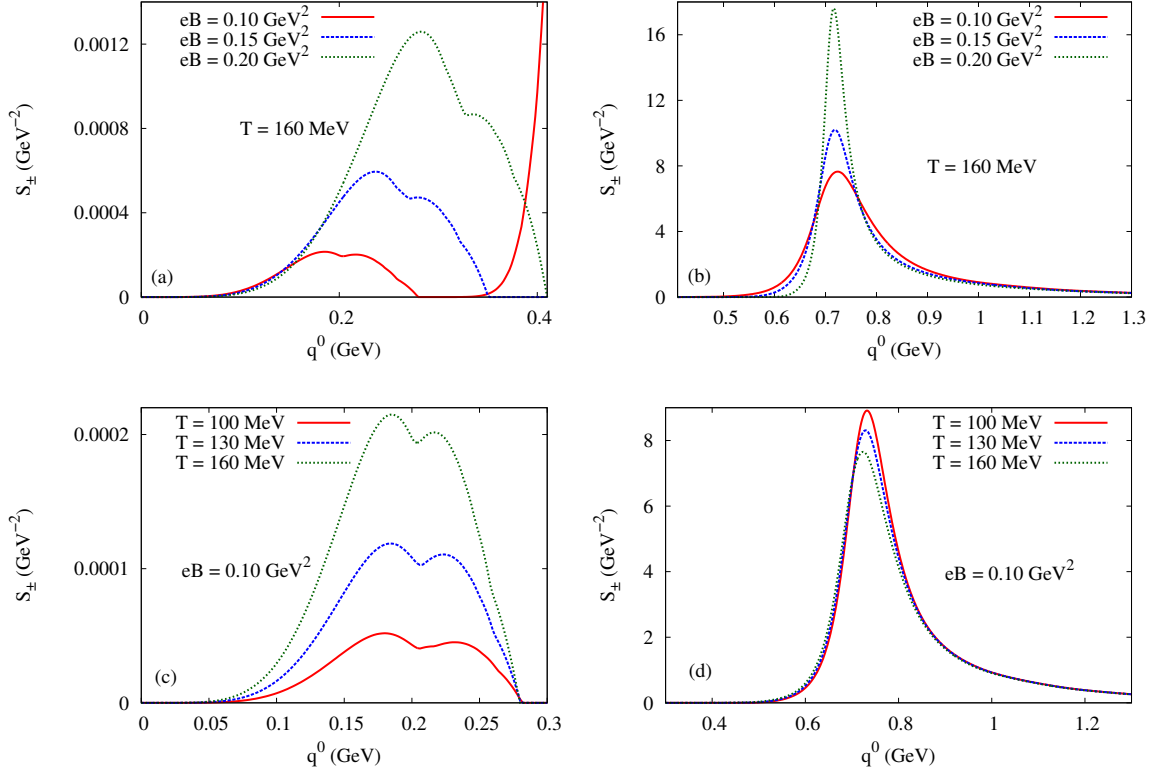


FIG. 10: The in-medium spectral functions of the  $\rho^\pm$  at constant temperature (160 MeV) and at three different values of the magnetic field (0.10, 0.15 and 0.20  $\text{GeV}^2$  respectively) (a) for  $q^0$  from 0 to 0.41 GeV (b) for  $q^0$  from 0.41 to 1.3 GeV (upper panel). The in-medium spectral functions of the  $\rho^\pm$  at constant magnetic field (0.10  $\text{GeV}^2$ ) and at three different values of the temperature (100, 130 and 160 MeV respectively) (c) for  $q^0$  from 0 to 0.30 GeV (d) for  $q^0$  from 0.30 to 1.3 GeV (lower panel).

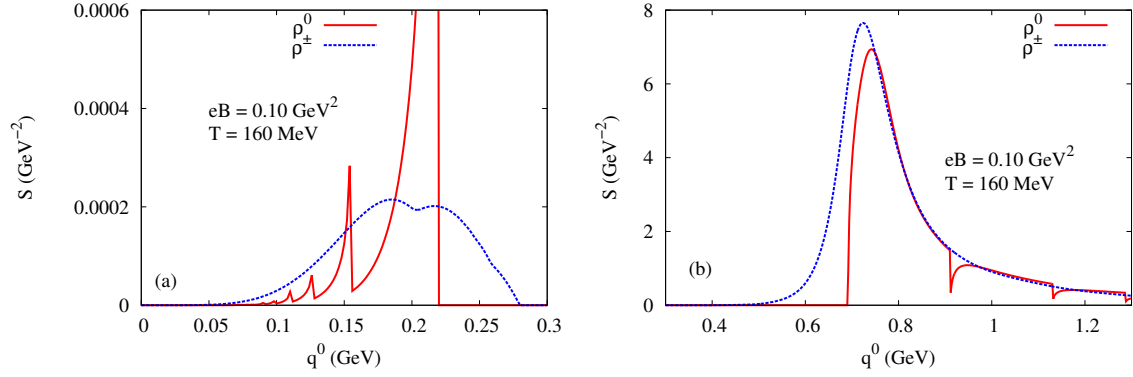


FIG. 11: The comparison of in-medium spectral functions between  $\rho^0$  and  $\rho^\pm$  at  $eB = 0.10 \text{ GeV}^2$  and  $T = 160 \text{ MeV}$  (a) for  $q^0$  from 0 to 0.30 GeV (a) for  $q^0$  from 0.30 to 1.3 GeV.

## VII. SUMMARY AND DISCUSSIONS

We have calculated the self energies of  $\rho$  meson using effective  $\rho\pi\pi$  interaction at finite temperature and arbitrary external magnetic field taking all the Landau levels in our calculations. The kinematic domains of the imaginary part of the self energy in the complex  $q^0$  plane is shown to be different for  $\rho^0$  and  $\rho^\pm$  as well as from the  $eB = 0$  case. For the vanishing three momentum of the  $\rho$ , we have observed Landau cut contributions to the imaginary part of

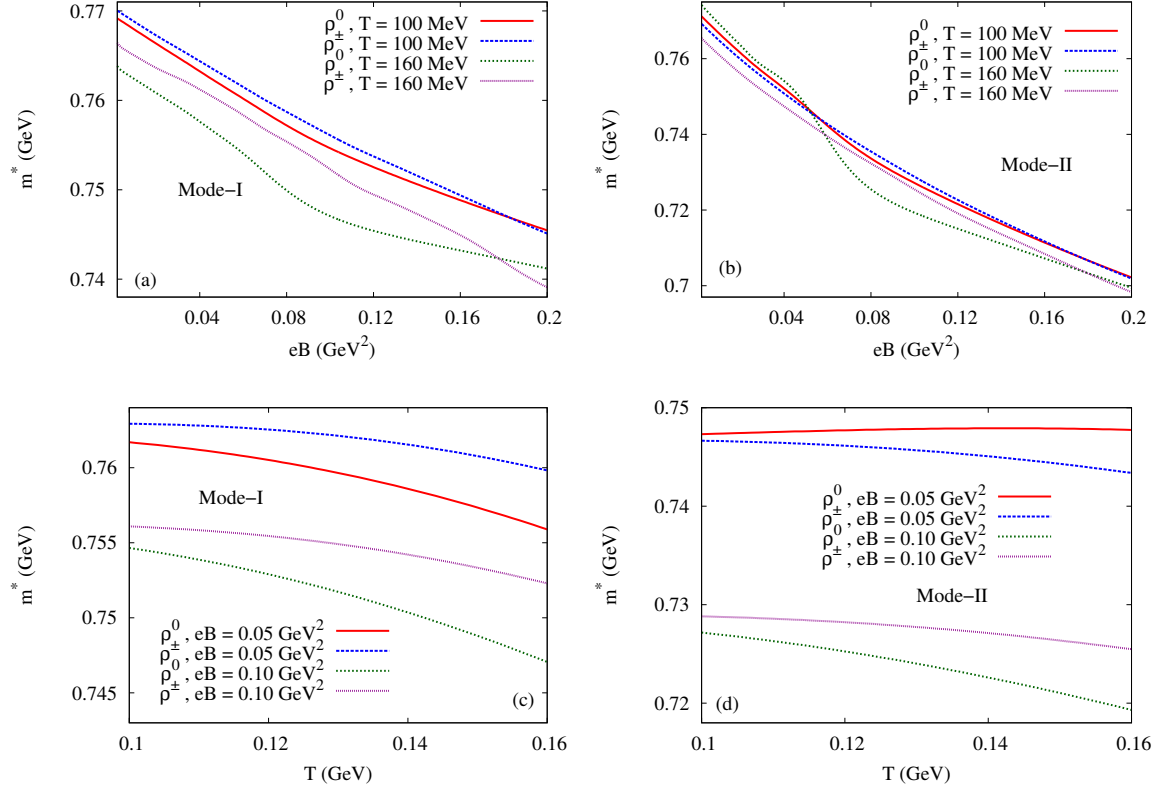


FIG. 12: The effective masses of the  $\rho$  vs  $eB$  at two different values of temperatures (100 and 160 MeV) for (a) Mode-I and (b) Mode-II. The effective masses of the  $\rho$  vs  $T$  at two different values of the magnetic field (0.05 and 0.1 GeV<sup>2</sup>) for (c) Mode-I and (d) Mode-II.

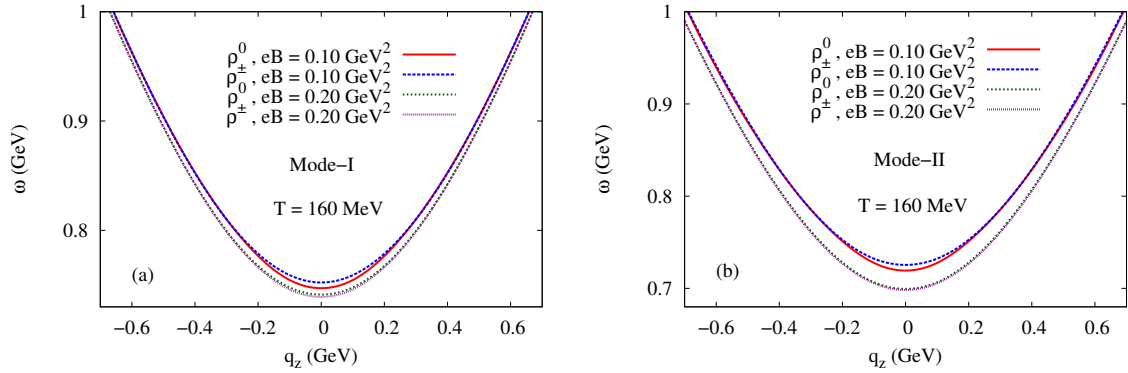


FIG. 13: The dispersion curve of the  $\rho$  at constant temperature (160 MeV) and at two different values of the magnetic field (0.1 and 0.20 GeV<sup>2</sup> respectively) for (a) Mode-I and (b) Mode-II.

the self energy at non-zero magnetic field which is absent at zero magnetic field. While calculating the real part of the self energy, we have taken the magnetic field dependent vacuum contributions which is usually ignored in most of the works in the literature and this term produces dominating effects in terms of the effective mass and dispersion relations. The in-medium spectral functions obtained from the spin-averaged self energy is shown to be quite different for  $\rho^0$  and  $\rho^\pm$ . The “Threshold Singularities” in the  $\rho^0$  spectral function give rise to spike like structures which is absent in case of  $\rho^\pm$ . It is also shown quantitatively that, the  $\rho$  meson melts at high magnetic field. This ‘melting’ occurs at respectively lower value of magnetic field for  $\rho^0$  as compared to the  $\rho^\pm$ . From the pole of the complete  $\rho$

propagator, we have evaluated its effective mass and dispersion relations. We find two distinct physical modes. The effective mass of  $\rho$  is seen to decrease with the increase in magnetic field as well as temperature.

### Acknowledgement

Snigdha Ghosh acknowledges Center for Nuclear Theory, VECC and Department of Atomic Energy, Government of India for support.

### Appendix A: Calculation of $\text{Re}(\Pi_0^{\mu\nu})_B$

We have

$$\begin{aligned} (\Pi_0^{\mu\nu})_B &= i \int \frac{d^4 k}{(2\pi)^4} \mathcal{N}^{\mu\nu} \Delta_B(k) \Delta_B(p = q - k) \\ &= i \int \frac{d^4 k}{(2\pi)^4} \mathcal{N}^{\mu\nu} \sum_{l=0}^{\infty} \sum_{n=0}^{\infty} \left[ \frac{\phi_l(\alpha_k) \phi_n(\alpha_k)}{(k_{\parallel}^2 - m_l^2 + i\epsilon)(p_{\parallel}^2 - m_n^2 + i\epsilon)} \right]. \end{aligned}$$

Using standard Feynman parametrization, we combine the denominators of the two propagators and obtain

$$(\Pi_0^{\mu\nu})_B = i \sum_{l=0}^{\infty} \sum_{n=0}^{\infty} \int_0^1 dx \int \frac{d^2 k_{\perp}}{(2\pi)^2} \phi_l(\alpha_k) \phi_n(\alpha_k) \int \frac{d^2 k_{\parallel}}{(2\pi)^2} \frac{\mathcal{N}^{\mu\nu}}{[(k_{\parallel} - xq_{\parallel})^2 - \Delta_{n,l}]^2},$$

where,  $\Delta_{n,l} = \Delta + eB(2l + 1 - 2xl + 2xn)$ . Shifting momenta  $k_{\parallel} \rightarrow (k_{\parallel} + xq_{\parallel})$  and performing the  $k_{\parallel}$  integration using dimensional regularization we get,

$$\begin{aligned} (\Pi_0^{\mu\nu})_B &= \left( \frac{g_{\rho\pi\pi}^2 q_{\parallel}^2}{4\pi} \right) i \sum_{l=0}^{\infty} \sum_{n=0}^{\infty} \int_0^1 dx \int \frac{d^2 k_{\perp}}{(2\pi)^2} \phi_l(\alpha_k) \phi_n(\alpha_k) \left[ \left( q_{\parallel}^2 g_{\parallel}^{\mu\nu} - q^{\mu} q^{\nu} \right) \frac{1}{2} \Gamma \left( 1 - \frac{d}{2} \right) \left( \frac{1}{\Delta_{n,l}} \right)^{1-d/2} \right. \\ &\quad \left. - q_{\parallel}^2 k_{\perp}^{\mu} k_{\perp}^{\nu} \Gamma \left( 2 - \frac{d}{2} \right) \left( \frac{1}{\Delta_{n,l}} \right)^{2-d/2} \right]_{d \rightarrow 2}. \end{aligned}$$

Now using the  $\overline{\text{MS}}$  scheme we subtract out the divergence arising from the pole of the Gamma function. The remaining  $k_{\perp}$  integration is convergent and can be evaluated using the orthogonality properties of the Laguerre polynomials present in the numerator which also remove one sum from the double sum. Then the  $(\Pi_0^{\mu\nu})_B$  can be written in the following compact form

$$(\Pi_0^{\mu\nu})_B = \left( \frac{g_{\rho\pi\pi}^2 q_{\parallel}^2}{32\pi^2} \right) \int dx \left[ \left( q_{\parallel}^2 g_{\parallel}^{\mu\nu} - q^{\mu} q^{\nu} \right) S_{\parallel} + q_{\parallel}^2 g_{\perp}^{\mu\nu} S_{\perp} \right] \quad (\text{A1})$$

where,  $S_{\parallel}$  and  $S_{\perp}$  are given by,

$$S_{\parallel} = \sum_{n=0}^{\infty} \left[ 2eB \ln \left( \frac{\Delta_{n,n}}{\mu_0} \right) \right] \quad (\text{A2})$$

$$S_{\perp} = \sum_{n=0}^{\infty} eB \left[ \frac{2n+1}{\Delta_{n,n}} + \frac{2n+2}{\Delta_{n+1,n}} \right]. \quad (\text{A3})$$

The infinite sums in Eq. (A2) and (A3) are divergent and can be regularized using "Derivative Regularization" technique [40]. To do this we differentiate them with respect to  $M = q_{\parallel}^2$  twice and obtain convergent sums, which are

expressible in terms of polygamma functions ( $\Psi$ ,  $\Psi'$  and  $\Psi''$ ),

$$\left(\frac{\partial^2 S_{\parallel}}{\partial M^2}\right) = \frac{-x^2(1-x)^2}{2eB} \Psi' \left(\frac{\Delta}{2eB} + \frac{1}{2}\right) \quad (\text{A4})$$

$$\begin{aligned} \left(\frac{\partial^2 S_{\perp}}{\partial M^2}\right) &= \frac{x^2(1-x)^2}{2(eB)^2} \left[ \Psi' \left(\frac{\Delta}{2eB} + \frac{1}{2}\right) + \left(\frac{\Delta}{4eB}\right) \Psi'' \left(\frac{\Delta}{2eB} + \frac{1}{2}\right) + \right. \\ &\quad \left. \Psi' \left(\frac{\Delta}{2eB} + \frac{1}{2} + x\right) + \left(\frac{\Delta}{4eB} + \frac{2x-1}{4}\right) \Psi'' \left(\frac{\Delta}{2eB} + \frac{1}{2} + x\right) \right]. \end{aligned} \quad (\text{A5})$$

Integrating Eq. (A4) and (A5), and substituting  $S_{\parallel}$  and  $S_{\perp}$  into Eq. (A1), we obtain,

$$\begin{aligned} (\Pi_0^{\mu\nu})_B &= \left(\frac{g_{\rho\pi\pi}^2 q_{\parallel}^2}{32\pi^2}\right) \int dx \left[ \left(q_{\parallel}^2 g_{\parallel}^{\mu\nu} - q^{\mu} q^{\nu}\right) \left(2eB \ln \Gamma \left(\frac{\Delta}{2eB} + \frac{1}{2}\right) + C_1 q_{\parallel}^2 + C_2\right) \right. \\ &\quad \left. + q_{\parallel}^2 g_{\perp}^{\mu\nu} \left(\frac{\Delta}{2eB} \Psi \left(\frac{\Delta}{2eB} + \frac{1}{2}\right) + \left(\frac{\Delta}{2eB} - \frac{1}{2} + x\right) \Psi \left(\frac{\Delta}{2eB} + \frac{1}{2} + x\right) + C_3 q_{\parallel}^2 + C_4\right) \right] \end{aligned} \quad (\text{A6})$$

where  $C_1$ ,  $C_2$ ,  $C_3$  and  $C_4$  are integration constants and independent of  $q_{\parallel}^2$  but can be functions of  $x$  and  $eB$ . These constants have to be chosen such that in the limit of zero magnetic field, we get back the vacuum self energy as given in Eq. (5) i.e.

$$\lim_{eB \rightarrow 0} (\Pi_0^{\mu\nu})_B = (\Pi^{\mu\nu})_{vac}. \quad (\text{A7})$$

From Eq. (A7), we get  $C_1 = C_3 = -x(1-x) \ln \left(\frac{2eB}{\mu_0}\right)$ ,  $C_2 = m^2 \ln \left(\frac{2eB}{\mu_0}\right)$  and  $C_4 = m^2 \ln \left(\frac{2eB}{\mu_0}\right) - m^2$ . Substituting the values of  $C_1, C_2, C_3$  and  $C_4$  into Eq. (A6) and taking the real part, we get Eq. (19).

## Appendix B: Calculation of $\text{Re}(\Pi_{\pm}^{\mu\nu})_B$

We have

$$\begin{aligned} (\Pi_{\pm}^{\mu\nu})_B &= i \int \frac{d^4 k}{(2\pi)^4} \mathcal{N}^{\mu\nu} \Delta_0(k) \Delta_B(p = q - k) \\ &= i \int \frac{d^4 k}{(2\pi)^4} \mathcal{N}^{\mu\nu} \sum_{n=0}^{\infty} \left[ \frac{\phi_n(\alpha_k)}{(k^2 - m_{\pi}^2 + i\epsilon)(p_{\parallel}^2 - m_n^2 + i\epsilon)} \right]. \end{aligned}$$

Using standard Feynman parametrization, we combine the denominators of the two propagators and obtain

$$(\Pi_{\pm}^{\mu\nu})_B = i \sum_{n=0}^{\infty} \int_0^1 dx \int \frac{d^2 k_{\perp}}{(2\pi)^2} \phi_n(\alpha_k) \int \frac{d^2 k_{\parallel}}{(2\pi)^2} \frac{\mathcal{N}^{\mu\nu}}{[(k_{\parallel} - xq_{\parallel})^2 - \Delta_n]^2},$$

where,  $\Delta_n = \Delta + x(2n+1)eB - (1-x)k_{\perp}^2$ . Shifting momentum  $k_{\parallel} \rightarrow (k_{\parallel} + xq_{\parallel})$  and performing the  $k_{\parallel}$  integration using dimensional regularization we get,

$$\begin{aligned} (\Pi_{\pm}^{\mu\nu})_B &= \left(\frac{g_{\rho\pi\pi}^2 q_{\parallel}^2}{4\pi}\right) i \sum_{n=0}^{\infty} \int_0^1 dx \int \frac{d^2 k_{\perp}}{(2\pi)^2} \phi_n(\alpha_k) \left[ \left(q_{\parallel}^2 g_{\parallel}^{\mu\nu} - q^{\mu} q^{\nu}\right) \frac{1}{2} \Gamma \left(1 - \frac{d}{2}\right) \left(\frac{1}{\Delta_n}\right)^{1-d/2} \right. \\ &\quad \left. - q_{\parallel}^2 k_{\perp}^{\mu} k_{\perp}^{\nu} \Gamma \left(2 - \frac{d}{2}\right) \left(\frac{1}{\Delta_n}\right)^{2-d/2} \right]_{d \rightarrow 2}. \end{aligned}$$

Now as before we subtract out the divergence arising from the pole of the Gamma function. The remaining  $k_{\perp}$  integration is converted to  $\alpha_k$  integration using  $d^2 k_{\perp} = (\pi eB) d\alpha_k$  getting,

$$(\Pi_{\pm}^{\mu\nu})_B = \left(\frac{g_{\rho\pi\pi}^2 q_{\parallel}^2}{32\pi^2}\right) \int_0^1 dx \int_0^{\infty} d\alpha_k \left[ \left(q_{\parallel}^2 g_{\parallel}^{\mu\nu} - q^{\mu} q^{\nu}\right) \tilde{S}_{\parallel} + q_{\parallel}^2 g_{\perp}^{\mu\nu} \tilde{S}_{\perp} \right] \quad (\text{B1})$$

where,  $\tilde{S}_\parallel$  and  $\tilde{S}_\perp$  are given by,

$$\tilde{S}_\parallel = \sum_{n=0}^{\infty} \left[ eB \phi_n(\alpha_k) \ln \left( \frac{\Delta_n}{\mu_0} \right) \right] \quad (\text{B2})$$

$$\tilde{S}_\perp = \sum_{n=0}^{\infty} \left[ \alpha_k (eB)^2 \frac{\phi_n(\alpha_k)}{\Delta_n} \right]. \quad (\text{B3})$$

Differentiating Eq. (B2) with respect to  $q_\parallel^2$ , we get,

$$\frac{\partial \tilde{S}_\parallel}{\partial q_\parallel^2} = \sum_{n=0}^{\infty} \left[ -x(1-x) \alpha_k (eB)^2 \frac{\phi_n(\alpha_k)}{\Delta_n} \right]. \quad (\text{B4})$$

The evaluate the infinite sums in Eq. (B3) and (B4), we have introduced a new parameter  $z$  and write

$$\frac{1}{\Delta_n} = \int_0^1 \frac{dz}{m_\pi^2} z^{\Delta_n/m_\pi^2 - 1}. \quad (\text{B5})$$

Substituting Eq. (B5) into Eq. (B3) and (B4) and using the identity  $\sum_{n=0}^{\infty} L_n(t) z^n = (1-z)^{-1} \exp\left(\frac{tz}{z-1}\right)$ , we obtain,

$$\tilde{S}_\parallel = eB \int_0^1 \frac{dz}{\ln z} z^{\Delta/m_\pi^2 - 1} \text{sech} \left( x \frac{eB}{m_\pi^2} \ln z \right) \exp(\zeta \alpha_k) + \tilde{C}_1 \quad (\text{B6})$$

$$\tilde{S}_\perp = \alpha_k (eB)^2 \int_0^1 \frac{dz}{m_\pi^2} z^{\Delta/m_\pi^2 - 1} \text{sech} \left( x \frac{eB}{m_\pi^2} \ln z \right) \exp(\zeta \alpha_k) \quad (\text{B7})$$

where,  $\tilde{C}_1$  is the constant of the  $q_\parallel^2$ -integration and is independent of  $q_\parallel^2$  which is chosen to be zero and

$$\zeta = (1-x) \frac{eB}{m_\pi^2} \ln z + \tanh \left( x \frac{eB}{m_\pi^2} \ln z \right). \quad (\text{B8})$$

Substituting Eq. (B6) and (B7) into Eq. (B1) and performing the  $\alpha_k$  integration we get,

$$(\Pi_\pm^{\mu\nu})_B = \left( \frac{g_{\rho\pi\pi}^2 q_\parallel^2}{32\pi^2} \right) \int_0^1 \int_0^1 dx dz z^{\Delta/m_\pi^2 - 1} \text{sech} \left( x \frac{eB}{m_\pi^2} \ln z \right) \left[ \left( q_\parallel^2 g_\parallel^{\mu\nu} - q^\mu q^\nu \right) \frac{eB}{\zeta \ln z} + q_\parallel^2 g_\perp^{\mu\nu} \frac{(eB)^2}{m_\pi^2 \zeta^2} \right] \quad (\text{B9})$$

In the limit of zero magnetic field, we get back the vacuum self energy as given in Eq. (5), i.e.

$$\lim_{eB \rightarrow 0} (\Pi_\pm^{\mu\nu})_B = \left( \frac{g_{\rho\pi\pi}^2 q_\parallel^2}{32\pi^2} \right) \left( q_\parallel^2 g^{\mu\nu} - q^\mu q^\nu \right) \int_0^1 dx \int_0^1 dz z^{\Delta/m_\pi^2 - 1} \frac{m_\pi^2}{(\ln z)^2} = (\Pi^{\mu\nu})_{vac}. \quad (\text{B10})$$

Using Eq. (B9) and (B10), we arrive at Eq. (21).

### Appendix C: Kinematic Domains of the Imaginary Parts

The imaginary part of the in-medium  $\rho$  self energy function at *zero magnetic field* in Eq. (14) contains four Dirac delta functions namely  $\delta(q^0 \mp \omega_k \mp \omega_p) = \delta(q^0 \mp E)$  and  $\delta(q^0 \mp \omega_k \pm \omega_p) = \delta(q^0 \mp E')$ , where  $E = \omega_k + \omega_p$  and  $E' = \omega_k - \omega_p$ . The functions  $E = E(|\vec{k}|, \cos \theta)$  and  $E' = E'(|\vec{k}|, \cos \theta)$  both are defined in the domain  $0 \leq |\vec{k}| < \infty$  and  $|\cos \theta| \leq 1$ . In this given domain the ranges of this two functions are found to be,

$$\sqrt{\vec{q}^2 + 4m_\pi^2} \leq E < \infty \quad \text{and} \quad -|\vec{q}| \leq E' \leq 0 \quad (\text{C1})$$



respectively. So, from Eq. (C1) it is evident that, for  $\delta(q^0 - E)$  and  $\delta(q^0 + E)$  to be non-vanishing, we must have  $\sqrt{q_z^2 + 4m_\pi^2} \leq q^0 < \infty$  and  $-\infty < q^0 \leq -\sqrt{q_z^2 + 4m_\pi^2}$  respectively. Similarly for  $\delta(q^0 - E')$  and  $\delta(q^0 + E')$  to be non-vanishing, we must have  $-|\vec{q}| \leq q^0 \leq 0$  and  $0 \leq q^0 \leq |\vec{q}|$  respectively.

The imaginary part of the in-medium  $\rho^0$  self energy function at *non-zero magnetic field* in Eq. (20) contains four Dirac delta functions in a particular set of Landau levels  $\{n, l\}$  namely  $\delta(q^0 \mp \omega_k^l \mp \omega_p^n) = \delta(q^0 \mp E_{n,l})$  and  $\delta(q^0 \mp \omega_k^l \pm \omega_p^n) = \delta(q^0 \mp E'_{n,l})$ , where  $E_{n,l} = \omega_k^l + \omega_p^n$  and  $E'_{n,l} = \omega_k^l - \omega_p^n$ . The functions  $E_{n,l} = E_{n,l}(k_z)$  and  $E'_{n,l} = E'_{n,l}(k_z)$  both are defined in the domain  $-\infty < k_z < \infty$ . In this given domain the ranges of this two functions are found to be,

$$\sqrt{q_z^2 + (m_l + m_n)^2} \leq E_{n,l} < \infty \quad \text{and} \quad \min[q_z, E_{n,l}^\pm] \leq E'_{n,l} \leq \max[q_z, E_{n,l}^\pm] \quad (\text{C2})$$

where,  $E_{n,l}^\pm = \frac{(m_l - m_n)}{|m_l \pm m_n|} \sqrt{q_z^2 + (m_l \pm m_n)^2}$ . So from Eq. (C2), we find that, in a particular set of Landau levels  $\{n, l\}$ , for  $\delta(q^0 - E_{n,l})$  and  $\delta(q^0 + E_{n,l})$  to be non-vanishing, we must have  $\sqrt{q_z^2 + (m_l + m_n)^2} \leq q^0 < \infty$  and  $-\infty < q^0 \leq -\sqrt{q_z^2 + (m_l + m_n)^2}$  respectively. Similarly for  $\delta(q^0 - E'_{n,l})$  and  $\delta(q^0 + E'_{n,l})$  to be non-vanishing, we must have  $\min[q_z, E_{n,l}^\pm] \leq q^0 \leq \max[q_z, E_{n,l}^\pm]$  and  $-\max[q_z, E_{n,l}^\pm] \leq q^0 \leq -\min[q_z, E_{n,l}^\pm]$  respectively.

In Eq. (20), the indices  $l$  and  $n$  run from 0 to  $\infty$ . However for a particular value of  $l$ ,  $n$  can have only three values  $l-1$ ,  $l$  and  $l+1$  due to the presence of Kronecker delta function in Eq. (23). Hence, when these indices are summed over from  $0 \rightarrow \infty$ ,  $\delta(q^0 - \omega_k^l - \omega_p^n)$  and  $\delta(q^0 + \omega_k^l + \omega_p^n)$  will be non-vanishing at  $\sqrt{q_z^2 + 4(m_\pi^2 + eB)} < q^0 < \infty$  and  $-\infty < q^0 < -\sqrt{q_z^2 + 4(m_\pi^2 + eB)}$  respectively whereas, both  $\delta(q^0 - \omega_k^l + \omega_p^n)$  and  $\delta(q^0 + \omega_k^l - \omega_p^n)$  will be non-vanishing at  $|q^0| < \sqrt{q_z^2 + (\sqrt{m_\pi^2 + eB} - \sqrt{m_\pi^2 + 3eB})^2}$ .

The imaginary part of the in-medium  $\rho^\pm$  self energy function at non-zero magnetic field in Eq. (22) contains four Dirac delta functions for a particular Landau level  $n$  namely  $\delta(q^0 \mp \omega_k \mp \omega_p^n) = \delta(q^0 \mp E_n)$  and  $\delta(q^0 \mp \omega_k \pm \omega_p^n) = \delta(q^0 \mp E'_n)$ , where  $E_n = \omega_k + \omega_p^n$  and  $E'_n = \omega_k - \omega_p^n$ . The functions  $E_n = E_n(|\vec{k}|, \cos\theta)$  and  $E'_n = E'_n(|\vec{k}|, \cos\theta)$  both are defined in the domain  $0 \leq |\vec{k}| < \infty$  and  $|\cos\theta| \leq 1$ . In this domain the ranges of these two functions are found to be,

$$\sqrt{q_z^2 + (m_\pi + m_n)^2} \leq E_n < \infty \quad \text{and} \quad -\sqrt{q_z^2 + (m_\pi - m_n)^2} \leq E'_n \leq 0 \quad (\text{C3})$$

respectively. So from Eq. (C3), we find that, in a particular Landau level  $n$ , for  $\delta(q^0 - E_n)$  and  $\delta(q^0 + E_n)$  to be non-vanishing, we must have  $\sqrt{q_z^2 + (m_\pi + m_n)^2} \leq q^0 < \infty$  and  $-\infty < q^0 \leq -\sqrt{q_z^2 + (m_\pi + m_n)^2}$  respectively. Similarly, for  $\delta(q^0 - E'_n)$  and  $\delta(q^0 + E'_n)$  to be non-vanishing, we must have  $-\sqrt{q_z^2 + (m_\pi - m_n)^2} \leq q^0 \leq 0$  and  $0 \leq q^0 \leq \sqrt{q_z^2 + (m_\pi - m_n)^2}$  respectively.

In Eq. (22), the index  $n$  runs from 0 to  $\infty$  and when it is summed over,  $\delta(q^0 - \omega_k - \omega_p^n)$  and  $\delta(q^0 + \omega_k + \omega_p^n)$  will be non-vanishing at  $\sqrt{q_z^2 + (\sqrt{m_\pi^2 + eB} + m_\pi)^2} < q^0 < \infty$  and  $-\infty < q^0 < -\sqrt{q_z^2 + (\sqrt{m_\pi^2 + eB} + m_\pi)^2}$  respectively whereas,  $\delta(q^0 - \omega_k + \omega_p^n)$  and  $\delta(q^0 + \omega_k - \omega_p^n)$  will be non-vanishing at  $0 < q^0 < \infty$  and  $-\infty < q^0 < 0$  respectively.

#### Appendix D: Simplification of the Imaginary Parts

The imaginary part of in-medium self energy function of  $\rho$  at zero magnetic field in Eq. (14) can be written as,

$$\text{Im } \bar{\Pi}^{\mu\nu}(q) = -\pi\epsilon(q^0) \int_0^\infty \int_0^\pi \int_0^{2\pi} \frac{|\vec{k}|^2 \sin\theta d|\vec{k}| d\theta d\phi}{(2\pi)^3 4\omega_k \omega_p} \left[ U_1(q, \vec{k}) \delta(q^0 - \omega_k - \omega_p) + U_2(q, \vec{k}) \delta(q^0 + \omega_k + \omega_p) \right. \\ \left. L_1(q, \vec{k}) \delta(q^0 + \omega_k - \omega_p) + L_2(q, \vec{k}) \delta(q^0 - \omega_k + \omega_p) \right], (\text{D1})$$

where,

$$\begin{aligned}
U_1 &= (1 + \eta^k + \eta^p) \mathcal{N}^{\mu\nu} (q, k^0 = \omega_k, \vec{k}) \\
U_2 &= (-1 - \eta^k - \eta^p) \mathcal{N}^{\mu\nu} (q, k^0 = -\omega_k, \vec{k}) \\
L_1 &= (\eta^k - \eta^p) \mathcal{N}^{\mu\nu} (q, k^0 = -\omega_k, \vec{k}) \\
L_2 &= (-\eta^k + \eta^p) \mathcal{N}^{\mu\nu} (q, k^0 = \omega_k, \vec{k})
\end{aligned}$$

For simplicity, we have taken  $\vec{q} = \vec{0}$  and it is to be noted that, the nonzero components of  $\mathcal{N}^{\mu\nu} (q^0, \vec{q} = \vec{0}, \vec{k})$  are independent of  $\theta$  and  $\phi$ . In Appendix (C) it is shown that, for  $\vec{q} = \vec{0}$  only Unitary terms contribute. So Eq. (D1) simplifies to,

$$\begin{aligned}
\text{Im } \bar{\Pi}^{\mu\nu}(q^0) &= \frac{-\epsilon(q^0)}{8\pi} \int_0^\infty \frac{|\vec{k}|^2 d|\vec{k}|}{\omega_k^2} \left[ U_1(q^0, |\vec{k}|) \delta(q^0 - 2\omega_k) \Theta(q^0 - 2m_\pi) \right. \\
&\quad \left. + U_2(q^0, |\vec{k}|) \delta(q^0 + 2\omega_k) \Theta(-q^0 - 2m_\pi) \right].
\end{aligned}$$

Transforming the Dirac delta functions  $\delta(q^0 \mp 2\omega_k) = \left(\frac{\omega_k}{2|\vec{k}|}\right) \delta(|\vec{k}| - \tilde{k})$  where  $\tilde{k} = \left(\frac{1}{2q^0}\right) \lambda^{1/2}(q_0^2, m_\pi^2, m_\pi^2)$  and performing the remaining  $|\vec{k}|$  integration we arrive at Eq. (24). Here  $\Theta(x)$  is the unit step function and  $\lambda(x, y, z) = (x^2 + y^2 + z^2 - 2xy - 2yz - 2zx)$  is the Kallen function.

The imaginary part of in-medium self energy function of  $\rho^0$  at non-zero magnetic field in Eq. (20) for  $\vec{q} = \vec{0}$  can be written as,

$$\begin{aligned}
\text{Im } \bar{\Pi}_0^{\mu\nu} &= -\pi\epsilon(q^0) \sum_{l=0}^\infty \sum_{n=0}^\infty \int_{-\infty}^{+\infty} \frac{dk_z}{(2\pi)} \frac{1}{4\omega_k^l \omega_k^n} \left[ U_1^{n,l}(q^0, k_z) \delta(q^0 - \omega_k^l - \omega_k^n) + U_2^{n,l}(q^0, k_z) \delta(q^0 + \omega_k^l + \omega_k^n) \right. \\
&\quad \left. + L_1^{n,l}(q^0, k_z) \delta(q^0 + \omega_k^l - \omega_k^n) + L_2^{n,l}(q^0, k_z) \delta(q^0 - \omega_k^l + \omega_k^n) \right]
\end{aligned}$$

where,

$$\begin{aligned}
U_1^{n,l} &= (1 + \eta_l^k + \eta_n^k) \mathcal{N}_{n,l}^{\mu\nu} (q, k^0 = \omega_k^l, k_z) \\
U_2^{n,l} &= (-1 - \eta_l^k - \eta_n^k) \mathcal{N}_{n,l}^{\mu\nu} (q, k^0 = -\omega_k^l, k_z) \\
L_1^{n,l} &= (\eta_l^k - \eta_n^k) \mathcal{N}_{n,l}^{\mu\nu} (q, k^0 = -\omega_k^l, k_z) \\
L_2^{n,l} &= (-\eta_l^k + \eta_n^k) \mathcal{N}_{n,l}^{\mu\nu} (q, k^0 = \omega_k^l, k_z)
\end{aligned}$$

Now we transform the Dirac delta functions  $\delta(q^0 \mp \omega_k^l \mp \omega_k^n) = \delta(q^0 \mp \omega_k^l \pm \omega_k^n) = \left(\frac{\omega_k^l \omega_k^n}{|k_z q^0|}\right) \left[\delta(k_z - \tilde{k}_z) + \delta(k_z + \tilde{k}_z)\right]$  where  $\tilde{k}_z = \left(\frac{1}{2q^0}\right) \lambda^{1/2}(q_0^2, m_l^2, m_n^2)$  and impose the kinematic domains as obtained in Appendix (C). After performing the  $k_z$  integration we arrive at Eq. (25).

The imaginary part of in-medium self energy function of  $\rho^\pm$  at non-zero magnetic field in Eq. (22) for  $\vec{q} = \vec{0}$  can be written as,

$$\begin{aligned}
\text{Im } \bar{\Pi}_\pm^{\mu\nu} &= -\pi\epsilon(q^0) \sum_{n=0}^\infty \int_0^\pi \int_0^\pi \frac{|\vec{k}|^2 \sin\theta d\theta}{(2\pi)^2} \frac{1}{4\omega_k \omega_k^n} \left[ U_1^n(q^0, |\vec{k}|, \theta) \delta(q^0 - \omega_k - \omega_k^n) + U_2^n(q^0, |\vec{k}|, \theta) \delta(q^0 + \omega_k + \omega_k^n) \right. \\
&\quad \left. + L_1^n(q^0, |\vec{k}|, \theta) \delta(q^0 + \omega_k - \omega_k^n) + L_2^n(q^0, |\vec{k}|, \theta) \delta(q^0 - \omega_k + \omega_k^n) \right] \quad (\text{D2})
\end{aligned}$$

where,

$$\begin{aligned}
U_1^n &= \phi_n(\alpha_k) (1 + \eta^k + \eta_n^k) \mathcal{N}^{\mu\nu} (q, k^0 = \omega_k, \vec{k}) \\
U_2^n &= \phi_n(\alpha_k) (-1 - \eta^k - \eta_n^k) \mathcal{N}^{\mu\nu} (q, k^0 = -\omega_k, \vec{k}) \\
L_1^n &= \phi_n(\alpha_k) (\eta^k - \eta_n^k) \mathcal{N}^{\mu\nu} (q, k^0 = -\omega_k, \vec{k}) \\
L_2^n &= \phi_n(\alpha_k) (-\eta^k + \eta_n^k) \mathcal{N}^{\mu\nu} (q, k^0 = \omega_k, \vec{k})
\end{aligned}$$

Now we transform the Dirac delta functions as bellow,

$$\begin{aligned}
\delta(q^0 - \omega_k \mp \omega_k^n) &= \left( \frac{\omega_k^n}{|\vec{k}|^2 \cos \theta_0} \right) \left[ \delta(\cos \theta - \cos \theta_0) + \delta(\cos \theta - \cos \theta_0) \right] \\
\delta(q^0 + \omega_k \mp \omega_k^n) &= \left( \frac{\omega_k^n}{|\vec{k}|^2 \cos \theta'_0} \right) \left[ \delta(\cos \theta - \cos \theta'_0) + \delta(\cos \theta - \cos \theta'_0) \right]
\end{aligned} \tag{D3}$$

where  $\cos \theta_0 = \frac{1}{|\vec{k}|} \sqrt{(q^0 + \omega_k)^2 - m_n^2}$  and  $\cos \theta'_0 = \frac{1}{|\vec{k}|} \sqrt{(q^0 - \omega_k)^2 - m_n^2}$ . Changing the variable of integration from  $|\vec{k}|$  to  $\omega_k$  and performing the  $\theta$  integration using the transformed Dirac delta function followed by imposing the kinematic domains as obtained in Appendix (C), Eq. (D2) becomes,

$$\begin{aligned}
\text{Im } \bar{\Pi}_{\pm}^{\mu\nu} &= \frac{-\epsilon(q^0)}{16\pi} \sum_{n=0}^{\infty} \int_{m_{\pi}}^{\infty} \frac{d\omega_k}{|\vec{k}|} \left[ \frac{\Theta(1 - \cos \theta_0)}{\cos \theta_0} \left( U_1^n(q^0, |\vec{k}|, \theta_0) + U_1^n(q^0, |\vec{k}|, -\theta_0) \right) \Theta(q^0 - m_{\pi} - m_n) \right. \\
&\quad + \frac{\Theta(1 - \cos \theta'_0)}{\cos \theta'_0} \left( U_2^n(q^0, |\vec{k}|, \theta'_0) + U_2^n(q^0, |\vec{k}|, -\theta'_0) \right) \Theta(-q^0 - m_{\pi} - m_n) \\
&\quad + \frac{\Theta(1 - \cos \theta'_0)}{\cos \theta'_0} \left( L_1^n(q^0, |\vec{k}|, \theta'_0) + L_1^n(q^0, |\vec{k}|, -\theta'_0) \right) \Theta(-q^0 - m_{\pi} + m_n) \Theta(q^0) \\
&\quad \left. + \frac{\Theta(1 - \cos \theta_0)}{\cos \theta_0} \left( L_2^n(q^0, |\vec{k}|, \theta_0) + L_2^n(q^0, |\vec{k}|, -\theta_0) \right) \Theta(q^0 - m_{\pi} + m_n) \Theta(-q^0) \right]. \tag{D4}
\end{aligned}$$

In Eq. (D4), the presence of the  $\Theta(1 - \cos \theta_0)$  and  $\Theta(1 - \cos \theta'_0)$  will further put restriction on the limits of the  $\omega_k$  integration and we will get Eq. (25).

- 
- [1] D. E. Kharzeev, K. Landsteiner, A. Schmitt and H. U. Yee, Lect. Notes Phys. **871**, 1 (2013) [arXiv:1211.6245 [hep-ph]].
  - [2] D. Kharzeev and A. Zhitnitsky, Nucl. Phys. A **797**, 67 (2007) [arXiv:0706.1026 [hep-ph]].
  - [3] D. E. Kharzeev, L. D. McLerran and H. J. Warringa, Nucl. Phys. A **803**, 227 (2008) [arXiv:0711.0950 [hep-ph]].
  - [4] K. Fukushima, D. E. Kharzeev and H. J. Warringa, Phys. Rev. D **78**, 074033 (2008) [arXiv:0808.3382 [hep-ph]].
  - [5] V. P. Gusynin, V. A. Miransky and I. A. Shovkovy, Nucl. Phys. B **462**, 249 (1996) [hep-ph/9509320].
  - [6] V. P. Gusynin, V. A. Miransky and I. A. Shovkovy, Nucl. Phys. B **563**, 361 (1999) [hep-ph/9908320].
  - [7] G. S. Bali, F. Bruckmann, G. Endrodi, Z. Fodor, S. D. Katz, S. Krieg, A. Schafer and K. K. Szabo, JHEP **1202**, 044 (2012) [arXiv:1111.4956 [hep-lat]].
  - [8] M. N. Chernodub, Phys. Rev. D **82**, 085011 (2010) [arXiv:1008.1055 [hep-ph]].
  - [9] M. N. Chernodub, Lect. Notes Phys. **871**, 143 (2013) [arXiv:1208.5025 [hep-ph]].
  - [10] V. Skokov, A. Y. Illarionov and V. Toneev, Int. J. Mod. Phys. A **24**, 5925 (2009) [arXiv:0907.1396 [nucl-th]].
  - [11] R. C. Duncan and C. Thompson, Astrophys. J. **392**, L9 (1992).
  - [12] E. J. Ferrer, V. de la Incera and C. Manuel, Phys. Rev. Lett. **95**, 152002 (2005) [hep-ph/0503162].
  - [13] E. J. Ferrer, V. de la Incera and C. Manuel, Nucl. Phys. B **747**, 88 (2006) [hep-ph/0603233].
  - [14] E. J. Ferrer and V. de la Incera, Phys. Rev. D **76**, 045011 (2007) [nucl-th/0703034 [NUCL-TH]].
  - [15] K. Fukushima and H. J. Warringa, Phys. Rev. Lett. **100**, 032007 (2008) [arXiv:0707.3785 [hep-ph]].
  - [16] B. Feng, D. Hou, H. c. Ren and P. p. Wu, Phys. Rev. Lett. **105**, 042001 (2010) [arXiv:0911.4997 [hep-ph]].
  - [17] S. Fayazbakhsh and N. Sadooghi, Phys. Rev. D **82**, 045010 (2010) [arXiv:1005.5022 [hep-ph]].
  - [18] S. Fayazbakhsh and N. Sadooghi, Phys. Rev. D **83**, 025026 (2011) [arXiv:1009.6125 [hep-ph]].

- [19] J. O. Andersen, W. R. Naylor and A. Tranberg, *Rev. Mod. Phys.* **88**, 025001 (2016) [arXiv:1411.7176 [hep-ph]].
- [20] K. l. Wang, S. x. Qin, Y. x. Liu, L. Chang, C. D. Roberts and S. M. Schmidt, *Phys. Rev. D* **86**, 114001 (2012) [arXiv:1209.2757 [nucl-th]].
- [21] C. Vafa and E. Witten, *Nucl. Phys. B* **234**, 173 (1984).
- [22] Y. Hidaka and A. Yamamoto, *Phys. Rev. D* **87**, no. 9, 094502 (2013) [arXiv:1209.0007 [hep-ph]].
- [23] M. N. Chernodub, *Phys. Rev. D* **86**, 107703 (2012) [arXiv:1209.3587 [hep-ph]].
- [24] C. Li and Q. Wang, *Phys. Lett. B* **721**, 141 (2013) [arXiv:1301.7009 [hep-th]].
- [25] M. N. Chernodub, *Phys. Rev. D* **89**, no. 1, 018501 (2014) [arXiv:1309.4071 [hep-ph]].
- [26] H. Liu, L. Yu and M. Huang, *Phys. Rev. D* **91**, no. 1, 014017 (2015) [arXiv:1408.1318 [hep-ph]].
- [27] M. Kawaguchi and S. Matsuzaki, *Phys. Rev. D* **93**, no. 12, 125027 (2016) [arXiv:1511.06990 [hep-ph]].
- [28] R. Rapp and J. Wambach, *Adv. Nucl. Phys.* **25**, 1 (2000) [hep-ph/9909229].
- [29] J. Alam, S. Sarkar, P. Roy, T. Hatsuda and B. Sinha, *Annals Phys.* **286**, 159 (2001) [hep-ph/9909267].
- [30] S. Mallik and S. Sarkar, *“Hadrons at Finite Temperature,”* Cambridge University Press.
- [31] S. Ghosh, S. Sarkar and S. Mallik, *Eur. Phys. J. C* **70**, 251 (2010) [arXiv:0911.3504 [hep-ph]].
- [32] J. Navarro, A. Sanchez, M. E. Tejeda-Yeomans, A. Ayala and G. Piccinelli, *Phys. Rev. D* **82**, 123007 (2010) [arXiv:1007.4208 [hep-ph]].
- [33] A. Ayala, A. Sanchez, G. Piccinelli and S. Sahu, *Phys. Rev. D* **71**, 023004 (2005) [hep-ph/0412135].
- [34] A. Bandyopadhyay, C. A. Islam and M. G. Mustafa, *Phys. Rev. D* **94**, no. 11, 114034 (2016) [arXiv:1602.06769 [hep-ph]].
- [35] J. C. D’Olive, J. F. Nieves and S. Sahu, *Phys. Rev. D* **67**, 025018 (2003) [hep-ph/0208146].
- [36] K. Hattori and K. Itakura, *Annals Phys.* **330**, 23 (2013) [arXiv:1209.2663 [hep-ph]].
- [37] M. Le Bellac, *“Thermal Field Theory,”* Cambridge University Press, Cambridge, England, 1996.
- [38] J. S. Schwinger, *Phys. Rev.* **82**, 664 (1951).
- [39] A. Ayala, C. A. Dominguez, L. A. Hernandez, M. Loewe, J. C. Rojas and C. Villavicencio, *Phys. Rev. D* **92**, no. 1, 016006 (2015) [arXiv:1504.01308 [hep-ph]].
- [40] M. D. Schwartz, *“Quantum Field Theory and the Standard Model,”* Cambridge University Press.